Method for Contactless Power Harvesting from Medium and High Voltage Power lines (11kV and above)

By

Hassan Pervaiz

Reg#00000170392

Session 2016-2019

Supervised by

Dr. Arsalan H. Khawaja

A Thesis Submitted to the US-Pakistan Center for Advanced Studies in Energy in partial fulfillment of the requirements for the degree of MASTERS of SCIENCE in Energy Systems Engineering

US-Pakistan Center for Advanced Studies in Energy (USPCAS-E)

National University of Sciences and Technology (NUST)

H-12, Islamabad 44000, Pakistan

June, 2019

THESIS ACCEPTANCE CERTIFICATE

Certified that final copy of MS thesis written by Mr. Hassan Pervaiz, (Registration No. 170392), of US-Pakistan Center for Advanced Studies in Energy (USPCAS-E) has been vetted by undersigned, found complete in all respects as per NUST Statues/Regulations, is within the similarity indices limit and is accepted as partial fulfillment for the award of MS degree. It is further certified that necessary amendments as pointed out by GEC members of the scholar have also been incorporated in the said thesis.

Signature: _____

Name of Supervisor _____

Date: _____

Signature (HoD): _____

Date: _____

Signature (Dean/Principal): _____

Date: _____

Certificate

This is to certify that work in this thesis has been carried out by **Mr. Hassan Pervaiz** and completed under my supervision in Smart Grid laboratory, US-Pakistan Center for Advanced Studies in Energy (USPCAS-E), National University of Sciences and Technology, H-12, Islamabad, Pakistan.

Supervisor: _____

Dr. Arsalan Habib Khawaja
USPCAS-E
NUST, Islamabad

GEC member # 1: _____

Dr. Kashif Imran
USPCAS-E
NUST, Islamabad

GEC member # 2: _____

Dr. Adeel Javed
USPCAS-E
NUST, Islamabad

GEC member # 3: _____

Dr. Syed Ali Abbas Kazmi
USPCAS-E
NUST, Islamabad

HoD- (dept) _____

Principal/ Dean _____

Dr. Zuhair S. Khan
USPCAS-E
NUST, Islamabad

DEDICATION

To my Parents, who supported me in every aspect of life.

ACKNOWLEDGMENTS

First and foremost, I am thankful to Almighty ALLAH who is the creator and author of knowledge. Indeed, without YOUR blessings, this mammoth task would not have been possible. And I acknowledge that without YOUR willingness and guidance, I would not have done a single task.

I am grateful to my parents for their unconditional love and sacrifices. I am forever in your debt for your encouragement, financial and moral support. Thank you for keeping confidence in me. I profusely thank my Sisters and Brother for cheering me up whenever i was down.

A special acknowledgment for my uncle, Umer Daraz, and his family for their support during my stay in Islamabad. Thanks to my Grandmother, relatives and Cousin who encouraged me throughout this span of life.

Sir Arsalan, I express my sincerest gratitude to you for this opportunity, for your teaching, mentorship and patience throughout the research. It has been truly a privilege to work with you.

I am also thankful to staff of Smart Grid Lab who helped and gave valuable advices during my experimentation

And to life, an extraordinary experience with so many things to enjoy within a short span. Thank you for giving me so much in the years past, and for more to discover in the years to come.

ABSTRACT

Sensing and Monitoring is critical for the Medium Voltage Transmission Lines (MVTLs) and High Voltage Transmission Lines (HVTLs) because of gradual degradation of power lines due to severe weather conditions and environment. This degradation of power lines causes undesired variations. Sensors are deployed to monitor the condition and variations of power lines. These sensors are powered up by batteries which need to be continuously replaced due to constraint of discharging. This occasional replacement of batteries can cause safety and life hazards due to their placement near the induction zone. The initial aim of research was to investigate a method for contactless energy harvesting and recharge these batteries without occasional replacement and going near induction zone of power lines to avoid life hazard. Inductive coupling was realized the best method to harvest energy near power lines. Power lines generate a region of magnetic field when current is passed through conductors. Inductive coil, using inductive coupling method, concentrates the magnetic field and converts it into Electrical energy. For making of inductive coil, ferromagnetic materials i.e. Mu-Metal, Silicon-Steel and Ferrite were comparatively analyzed with geometries like Cylindrical, Rectangular and Cone in ANSYS Maxwell Electromagnetism. The visual results of magnetic flux concentration showed that core of Mu-Metal cone is suitable for making inductive coil. A Mu-Metal cone-shaped coil was physically designed and tested in Laboratory under the magnetic Field region generated by Helmholtz coil. The coil was placed at the magnetic field density of 10uT which induced voltages of 1.25V. It was further connected to the energy harvesting circuit that was consisted of Multiplier circuit and Buffer circuit. When fully recharged, the end terminals showed the DC output of 650mV. The total coil resistance under magnetic field region was 90ohms at 3950 copper turns. Total power and power density achieved by the coil was 6mW and 5.5uW/cm^3 which is better than any previous designs using inductive coupling method.

Keywords: Energy Harvesting, Inductive Coupling, Mu-Metal, Cone-Shaped, Power lines

Table of Contents

List of Figures

List of Tables

List of Journals/Conference Papers

Conference Paper

- Hassan Pervaiz, Arsalan H. Khawaja "**Investigation on employability of High Magnetic Permeable Materials for energy harvesting application in high voltage power lines magnetic field zone**" in EESD 2018

Journal Paper

- Hassan Pervaiz, Arsalan H. Khawaja, Muhammad Kazim "**Method for Contactless Energy Harvesting Under Medium and High Voltage Power lines**" in Sensor Journal (To-be Subtmitted)

* Attached to Appendix A

List of Abbreviations

HVPL	High Voltage Power Lines
MVPL	Medium Voltage Power Lines
MF	Magnetic Field
EH	Energy Harvesting
EFEH	Electric Field Energy Harvesting
PEH	Piezoelectric Energy Harvesting
MFEH	Magnetic Field Energy Harvesting
MEMS	Microelectromechanical Systems
CT	Current Transformer
AC	Alternate Current
DC	Direct Current
PLM	Power Line Monitoring
CMU	Centralized Monitoring Unit
IoT	Internet of Things
FEA	Finite Element Analysis
CST	Computer Simulation Technology
Mn-Zn	Manganese-Zinc
IPLEH	Indoor Power lines based Magnetic Field Energy Harvester
WSN	Wireless Sensing Network
EEHC	Equivalent Energy Harvesting Circuit
SWG	Standard Wire Gauge
uT	Micro-Tesla
mT	Milli-Tesla
mW	Milli-Watts
uW	Micro-watts
mm	Millimeter

Chapter #1

INTRODUCTION

1.1 Background

The world has observed an enormous development in renewable energy generation techniques to address the problem of environmental changes. The exponential growth of world population has led in increase of power and electricity demand. Renewable energy is expected to penetrate and it is believed that it may require new medium and high voltage transmission lines. Energy demand is expected to accelerate in coming decades.

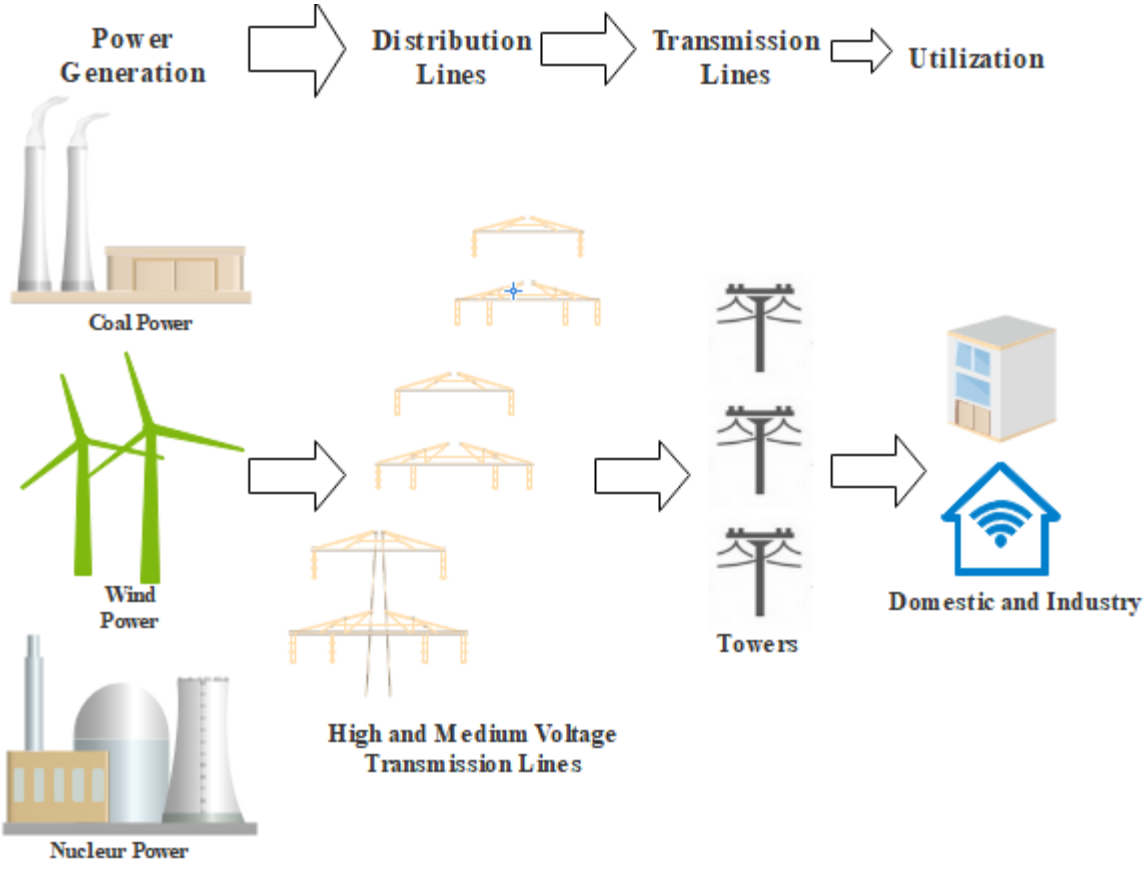

Figure 1.1: Power Distribution from source to end-users

Power delivery from power plants to domestic and industrial users cause load on transmission and power lines. Heavy load and gradual aging of transmission and power lines equipment are the main reason of power losses. The monitoring of power distribution transmission lines has become important issue in power system engineering because 85-

87% of power system faults are occurring in transmission lines [1]. The power lines monitoring is modernized concept to increase the efficacy and safety so that minimum energy is lost during power delivery. Implementation of such sensing and monitoring devices allow to properly and efficiently manage the transfer of electrical energy between the power generation source and the users.

Power line monitoring (PLM) is a notion that uses wireless communication network to a centralized unit to provide real-time status of power lines. The deployed wireless sensors deliver physical conditions such as gradual aging effects, broken lines and effects of severe environmental conditions in terms of temperature, overloading, heating, current and voltage to foresee the potential faults at the power lines.

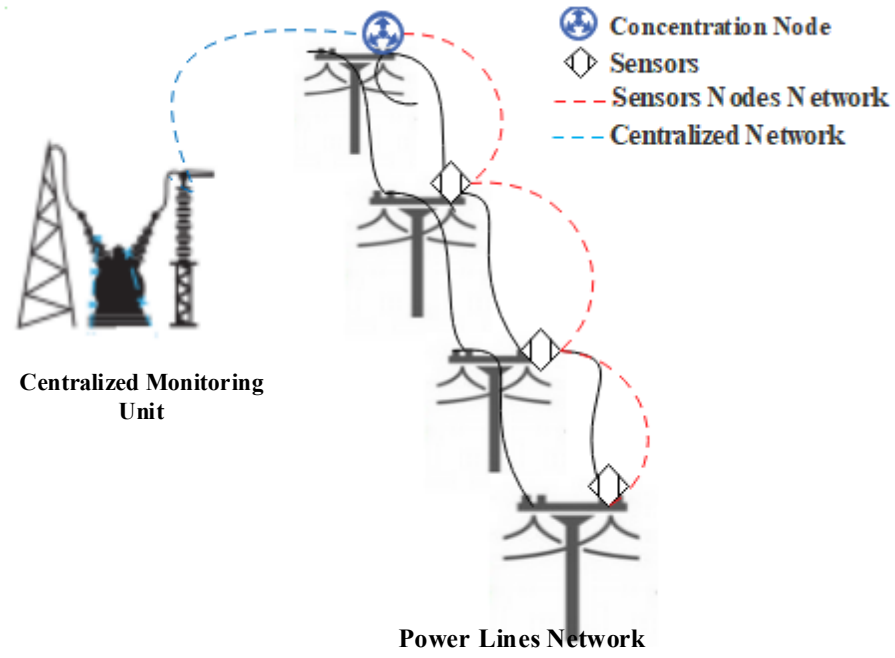

Figure 1.2: A distribution power line sensor network

Figure 1.2 depicts the sensor nodes located at the power lines. Each sensor node is connected to a centralized concentrating node which gathers data from every sensor and transmits information about condition of power lines to centralized monitoring unit. These sensor nodes are needed to spread over the large geographical range and a technology is

required that can power these larger distributed sensor nodes and that can able to self-power from the environment of power lines [2].

Sensor nodes have been conventionally powered up by the batteries that are deployed at the power lines. There are many conundrums with the usage of battery for powering the sensors such as the discharging, need of regular maintenance and replacement [3]. Replacement of battery is an effective solution for small IoT systems but for larger IoT network, it is not a feasible solution. Since the communication between IoT devices consume large amount of energy, devices operate only for limited duration because of finite battery capacity. Also maintenance and replacement of battery lead towards the safety and life hazards for the technicians. These constraints subject to develop a method that can either replace the battery or continuously recharge it. Energy harvesting has become an optimal solution for charging batteries and self-powering the sensor nodes in the power lines.

1.2 Energy Harvesting

In Energy Harvesting, energy is scavenged from external natural resources such as Solar, wind, vibrational and mechanical energy. A lot of technical development and research has been done in capturing energy from these sources and efficiently converting it into electrical energy. Since the power densities of these natural resources are not very large, they are used for low-power systems such as sensor nodes and other devices that operate at low power. Energy Harvesting (EH) techniques have grown exponentially with a growing interest in sensor nodes for Internet of Things (IoT) network and has become an attractive and promising solution for self-sustainable sensor nodes.

1.2.1 Solar Energy Harvesting

This process includes the capturing of radiated solar energy and converting this light energy into electrical energy. Energy is captured by solar panels which are placed at the region of sun-exposure. Although, solar energy is ambient and predictable, harvested energy is limited by sunlight availability. It has the highest power density of 15-100mW/cm^2 among other energy harvesting techniques [4]. These solar energy systems

can be utilized for monitoring of overhead power lines but with constraints like output power fluctuations and installation costs.

1.2.2 Piezoelectric Energy Harvesting

The technique involves converting the kinetic energy into electrical energy by using the piezoelectric effect, in which certain materials generate AC voltages when stress is applied on them. This energy is widely available but with the limitations of uncontrollability and unpredictability. The average power density of PEH is around 1mW/cm^3 with constraint of fluctuation and hard implementation [5].

1.2.3 Electric Field Energy Harvesting (EFEH):

When any conductor is energized with some voltage levels, the radial E-Field is produced. E-Field is present in abundance around the overhead Medium and High voltage power lines. Electrical energy is scavenged from Electric field of power lines through capacitive coupling method where energy is coupled from source to storage capacitors [6] Since the energy harvesting is done by inducing electric field when current carrying conductor is energized, this method can be called EFEH. Although, it is a non-ambient energy source but it is controllable and predictable [7]. EFEH can be applied to the power transmission lines and smart grids for monitoring applications.

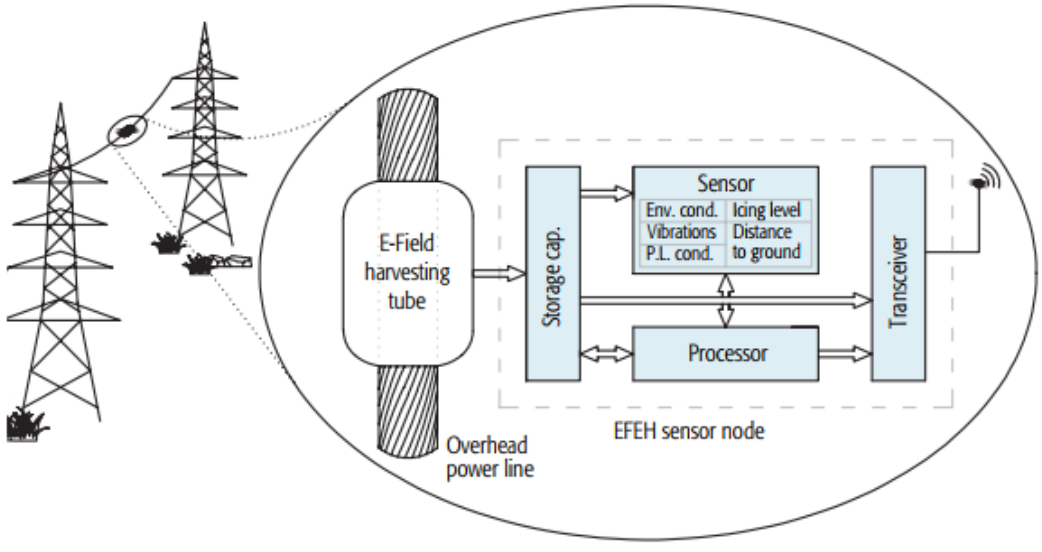

Figure 1.3: Practical Model Diagram of EFEH sensor nodes deployed at Power lines [8]

1.2.4 Magnetic Field Energy Harvesting (MFEH):

Energy harvesting from magnetic field is the most sought out and researched technique around power lines. MF originates when any conductor or equipment pass through a large current. Unlike EFEH, MF energy is scavenged by either current-transformer inductive coupling method or contactless inductive coupling. This technique involves a coil, which is made up of ferromagnetic core material which is then wound by copper wire. On placing the inductive coupling coil around any magnetic field region, energy is converted into electrical energy [9].

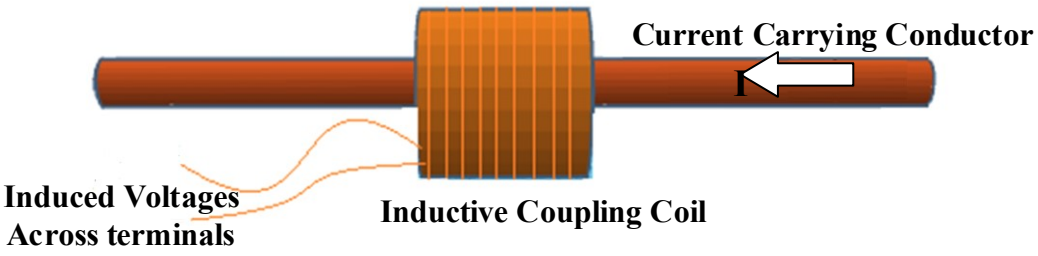

Fig 1.4: Diagram of Energy Harvesting by Contact-Transformer method around conductors

Conventionally, energy from magnetic fields around the high voltage power lines using current transformers (CTs) and energy derived from CT-based inductive couplers would be used for powering the power protection relays [10]. CT provides the better magnetic flux concentration in the coil since there is direct magnetic flux linkage with current carrying conductors. Coils are mounted around current carrying conductors as shown in Figure 1.4. Despite its good flux linkage, CT-based inductive coupling is not a good solution for HV power lines since coils are to be mounted around conductors which have higher cross sectional area than the typical CT transformer coils. Since CT-based inductive coupling require intrusive contact-based attachment to the conductors, it cause severe life hazard limitations for the technicians.

Figure 1.5 illustrates the typical energy harvesting from magnetic field, originated by power lines, by inductive coil. Current in the conductors of power lines generates the magnetic field in the surrounding.

Fig 1.5: Model Diagram of Energy Harvesting by Inductive Coupling method from Power Lines

Inductive coil couples with the magnetic field to generate magnetic flux in the coil which ultimately converts magnetic field into electrical energy. Contactless energy harvesting using magnetic field at some distance from power lines pose as a suitable candidate for powering up contactless sensors.

1.3 Problem Statement

In contact transformer inductive coupling, a strong magnetic flux linkage is generated with the inductive coil but with the contactless energy harvesting, flux linkage is not as robust. Magnetic field strength is the highest at center of power lines but as the distance is increased, the strength of magnetic field is decreased. When coil is placed at a distant away from current carrying conductors or power lines, magnetic field becomes linear which makes harder for inductive coupling device to concentrate magnetic flux. Taking account such constraints and conditions, it is admissible to look and investigate the parameters of coil that can enhance the magnetic flux linkage of inductive coil. The increase in magnetic flux linkage with the coil increases induced voltages which ultimately improve the power density.

1.4 Objectives

This thesis addresses the following objectives and research questions relating to Contactless Magnetic field energy harvesting.

1. What ferromagnetic material should be utilized as a core for inductive coil?

Any material that has higher magnetic permeability than air tends to concentrate the magnetic field. Ferromagnetic materials are differed from each other in terms of their ability to concentrate when they are placed in the region of magnetic field. This research will answer and find the right efficient, low-cost material can be utilized for the MFEH.

2. What will be the design or geometry of the core material for inductive coil?

Effective permeability is directly linked to voltage induction which is in relation with power density. So in order to achieve higher power density, effective permeability needs to be increased. Effective permeability is dependent upon core material and geometry. Core needs to have a geometry that can allow maximum number of magnetic field lines from itself under magnetic field region. The thesis will investigate different geometries for core by finite element analysis.

3. How are induced voltages, power and power density of the proposed method comparable to the other designs?

By making the inductive coil from using researched ferromagnetic core material and geometry, the results will be compared to the previous designs in order to answer the effectiveness and efficiency of the proposed method.

4. How can extracted energy be converted to utilize for the end products?

The power, that will be extracted from inductive coil, needs to be utilized by low-power devices. The thesis identifies method that can convert the scavenged energy for powering the compatible devices.

1.5 Thesis Overview

The content of each chapter in this thesis is outlines below.

Chapter 1 discusses the context of this research and give acquaintance with the research objectives of this work. This section also addresses the contribution made by this research in magnetic field energy harvesting.

Chapter 2 consists of Literature review on Energy harvesting by using inductive coupling method. This chapter analyze the past researches and studies done by Current-Transformer and Contact less methods for Magnetic Field Energy Harvesting and limitations of the previous designs.

Chapter 3 discusses the concepts and theory that are the basis of our research.

Chapter 4 introduces the software that will be used for Finite Element Analysis. It will be further sectioned into components of the software. This chapter will also consist of simulation environment and FEA results.

Chapter 5 takes account the simulation results into physical realization of the inductive coil. Every component of the proposed coil method will be briefly analyzed and discussed in this section.

Chapter 6 deals with the experimental analysis of proposed coil method. The section deals with the subjects other than proposed coil design under which it will be placed. A brief introduction of magnetic field generator, Helmholtz coil, and other measuring units will also be part of this section. It also consists of the energy harvesting circuit that will be connected to the harvesting coil. The section provides details and analyze the different sections of energy harvesting circuit.

Chapter 7 describes the results of experiments done by proposed coil and compares the results with the previous studies and designs.

Chapter 8 concludes the thesis. This section will review the contribution made by this research and suggestions for the future work in the field of magnetic field energy harvesting.

1.6 Contributions of this Research

This section presents the novel contribution made in this research in the field of Magnetic field energy harvesting.

The initial contribution of this research is to develop a MF energy harvesting coil. The proposed MF energy harvesting method in this thesis is contactless inductive coupling method that uses magnetic field as a source and couples with it, to harvest the energy. The parameters of the proposed coil are initially simulated and validated by experiment.

The second contribution in this field is to developing an energy harvesting circuit that can utilize the power extracted from coil into a proper manner. The end devices that can be utilized with contactless inductive coil are conditioning sensors, batteries and low-power operating devices.

The foremost contribution is the increase in the power density of proposed coil. The coil was able to achieve high powers under low volume. It is safe to say that proposed coil has the highest power density than previous designs and methods under contactless energy harvesting.

SUMMARY

Chapter 1 starts with the broader prospects that how world is going towards renewable energy from conventional energy sources. It follows with the integration of power distribution lines and smart monitoring system. A brief analysis on environmental problems faced by high voltage and medium voltage power lines, is also part of introduction. Introduction goes ahead with monitoring system and sensors which are deployed at the power lines. Some constraints related to conventional battery-based system and modern solutions are also discussed in this section. A brief overview of the energy harvesting techniques with energy extraction from magnetic field is part of this section.

Introduction section overviews the problems that will be addressed in this section. It also includes that how thesis is sectioned and ends while discussing the contribution this research made in the field of energy harvesting.

Chapter #2

LITERATURE REVIEW

Magnetic field energy harvesting (MFEH) is a very appealing choice for energy harvesting from the Medium-Voltage (MV) and High-Voltage (HV) power lines. Since, these power lines are source of uniform magnetic field, inductive coil obtains their energy from these lines. The interest in MFEH has spread over the last decade as the studies and researches on the field of inductive coupling and converting these studies into the compatible applications such as low-power electronic devices deployed near the power lines has significantly increased. The problem with the deployed sensors and devices is their inability to be self-sufficient in terms of power. Most of the literature review is done in the broader context of solving the power requirements for the batteries that power the sensors. Power can be directly delivered to sensors or indirectly to the batteries that are connected to sensor nodes. The collection of small amounts of energy (less than 1 W) from environmental sources such as power lines is the general topic of Literature review.

The past literature specifically has done in context of efficiently utilizing the Faraday's law of induction.

2.1 Solenoid-Coil

Roscoe et al. designed a contact-free energy harvester using inductive coupling method. Inductive coil, after theoretical analysis, was optimized to 50cm cast-iron solenoid-core with 40000 copper turns and was placed at the region of 18uT magnetic field density of 50Hz power frequency system. Coil was able to induced 10.5V and harvested power of 833uW on a matched-load of 33kΩ. Multiplier circuit was designed for further conversion of induced voltages into DC voltages while doubling the peak voltages. Buffer circuit was used to control and connect the rectified induced voltages with DC-DC converter. When there was sufficient magnetic flux linkage or induced voltages, buffer circuit passed through the induced voltage to DC-DC converter which further boosted-up DC voltages and ultimately powering up the conditioning sensors. This method achieved the power density of 5.5uW/cm^3 [11]. Cast-iron core based coil suffers great amount of eddy current

losses which is undesirable in this area. The length of coil is 0.5m which reduces its ability to achieve higher power densities.

2.2 Helical-Coil

Yuan et al. used the concept of increasing the path of magnetic flux and decreasing the demagnetizing factor for the making of inductive coil. A coil with Helical core was initially simulated and optimized in the CST software and then physically realized. The authors found out that Helical core increases the magnetic flux path inside the ferrite material. Coil was 15cm in length with 5 helical turns and had total volume of 273cm^3. On experimenting the coil with 400 copper turns, the total open circuit induced voltages were 185mV with power and power density of 612uW and 2.1uW/cm^3 respectively, when it was placed under the magnetic field density of 7uT. Authors predicted that power density could go as high as 7.9uW/cm^3 when number of copper turns increased to 2000 [12]. Although, the achieved power density is higher but the constraint of making a core in single piece remains which will prevent for making larger coils.

2.3 Bow-Tie Coil

The authors investigated a core design that can concentrate magnetic flux when it is placed under the magnetic field. A core of bow-tie geometry was modelled which was initially proved by simulation that it has lower demagnetization factor. A coil of Mn-Zn ferrite bow-tie coil was physically designed and experimented. Authors compared proposed designs with other existing design and gave each coil the length of 15cm with 100 enameled copper wire turns. They were placed in uniform magnetic field of 6uT, generated by Helmholtz coil. Results verified that Bow-tie coil achieved the least demagnetization factor, induced 2.95V. The total output power and power density were 360uW and 1.86uW/cm^3 at 40000 turns, which were better than any existing inductive coil designs [13]. The design of Bow-tie coil is complex and making the core by adjoining different piece cause eddy current losses.

2.4 Toroidal Core

Park et al. researched for the coil design on the basis of magnetic saturation effects which cause power degradation in harvester over time. Authors designed a toroidal core using Permeability H-curve and Ampere's circuital law for inducing the maximum voltages. It was determined that the inner radius of toroidal must be smaller to have higher induction of voltages. They combined the inner-radius toroidal parameter with the BH-curve of the core. The optimum distance between toroidal core and power lines was 15-20mm for inducing maximum voltages when it is clamped with the power lines. On further decreasing the inner radius, it was observed that saturation effects arise and induced voltages decreases. The toroidal core achieved induced voltages of 60.9V when distance between power line and toroidal core was 17.4mm [14]. The design can only be limited to lower cross-sectional current carrying conductors and it is not feasible with the overhead power lines.

2.5 Improved Energy Harvesting System

The authors presented a harvester design consisted of toroidal shape coil clamped around conductor carrying current of $10A_{rms}$ power lines. Harvesting coil was further connected with the management circuit that would release the power from capacitors once they were fully recharged as the instantaneous release of power is larger than average power. Coil induced 3.98V and total harvested power was 792mW at load resistance of 20Ω and for a duration of 110ms. [15].

2.6 Miniature Energy Harvesting Device

Bhuiyan et al. put forward a multi-layered-core coil energy harvesting device for powering the wireless sensors. Core materials were given intentional air-gaps so that they can enclose the power lines similar to a Rogowski coil. The width of single core layer was 0.1016mm which was increased by increasing the number of layers. Coil enclosed the conductor carrying current of 11.5A which caused coil to induce maximum of 1.4V. Results showed the linearity between the number of turns and width. Coil was further connected to the multiplier circuit which double the induced voltages to 2.4V. Maximum power obtained was 10.385mW at the load resistance of 76.09Ω [16].

2.7 Indoor Power lines based Magnetic Field Energy Harvester (IPLEH)

P.Maharjan et al. proposed an harvester device based on indoor power line energy harvesting. Initially, a design was simulated consisted of ferrite-based C-shaped split core in ANSYS Maxwell. Magnetic flux concentration was observed highest at the center and decreased as the distance increased from the center. Core was consisted with an outer diameter, inner diameter and height of 22cm, 13cm and 29mm respectively. It was clamped with current carrying power lines. Split core gave an advantage of easily wrapping around the current-carrying conductors. IPLEH was able to induce maximum of $9V_{rms}$ voltages when it was attached with conductor carrying current of 65.3A at 60Hz frequency. IPLEH, at maximum, delivered 105.24mW with the matched load-resistance of 230Ω. This design achieved the average power density of 14.67mW/cm^3. IPLEH successfully powered Wireless Sensing Network (WSN) which was further connected with the Bluetooth Module for real-time monitoring of the smart home. This design has constraint that it is only feasible with power lines with smaller cross-sectional area and not suitable for the overhead power lines because of their larger cross-sectional area [17].

2.8 Rectangular Coil

Z Wu et al presented a rectangular-shaped core coil which used contact-transformer inductive coupling method. An extra U-shaped electrical-steel sheet coil was placed near the rectangular shape to guide the magnetic flux towards the proposed rectangular-coil so that it can concentrate maximum magnetic field. Coil was given 1250 copper turns and had 2.78H of inductance and 107.6Ω of resistance. It was tested with different current carrying conductors and was able to extract a maximum of 230 milli-watts when placed at the $50A_{rms}$ [18].

2.9 X-Shaped Coil

The X-shaped magnetic flux concentrating ferromagnetic core was proposed by *Moghe et al.* Coil was developed 6cm long and were given the 300 turns of copper wire. It was then placed on the current carrying conductor of 900A. The coil induced 1.21V and harvest power of 29.8mW at maximum and achieved power density of 2.4mW/cm^3. Since the total volume of coil was low and number of copper turns were also low so constraint

of power density was aroused [19]. The authors did not provide the information about the ferromagnetic core material.

2.10 Magnetic Power Line Noise:

By using Brooks coil, a circular coil with square cross section, the air-core coil was designed by *Tashiro et al.* Coils were placed at the magnetic field density of 21.2uT at 60Hz frequency, 6.32mW of power could be harvested. Due to core design of Brooks coil, there were limitation of power density. Although, coil managed to have power density of 1.47uW/cm^3 [20]. Brooks coil are without ferromagnetic core materials that prevent the to achieve higher inductance values. For achieving the higher inductance values, coil needs to have more copper turns which ultimately cause higher copper losses in the coil.

SUMMARY

Literature Review explored the previous studies related to the field of energy harvesting and specifically to the extraction of energy from the magnetic field source. During literature review, it was observed that studies and researches are based on either contactless inductive coupling or contact-transformer based techniques. The main focus of researchers was to investigate methods so that power density of the inductive coil could be increased and that maximum power can be provided to batteries and sensor nodes. Specifically, core geometry, ferromagnetic material and optimization of other coil parameters were the subject of interest in these researches and studies. This section includes all the earlier and latest attempts made in this field and briefly discusses all of them.

CHAPTER#3

THEORY

3.1 Faraday's Law of Induction

In a contactless energy harvesting technique, a coil is made up of ferromagnetic materials that has capability to transduce the magnetic field energy that is located around High voltage power lines into electrical energy. In previous studies, researchers utilized the ability of ferromagnetic materials to permeabilize magnetic field lines and to lengthen the magnetic flux path inside material. These fundamental properties of ferromagnetic materials lead towards the increase in the voltage induction. According to Faraday's law of induction, whenever any conductor is placed in a magnetic field region, electromotive force or voltage is induced.

The center of our study is optimizing the feasible core material and design that possess the property of increased magnetic flux path and induce more voltages in lesser volume, according to the Faraday's law of induction [12].

$$V_{in} = N\omega B_{ex} A u_{eff} \qquad (1)$$

Where V_{in} is the voltages induced by the coil, N is the number of copper winding turns around the core, B_{ex} is the external magnetic field around the transmission lines, ω is the angular frequency of B in terms of radian/sec, A is the effective area of the coil and u_{eff} is effective permeability of coil which is normally related to the magnetic permeability of core material and geometric shape.

The core design mainly depends upon the effective permeability u_{eff}, that is further sub-divided into materialistic property and the geometry. High effective permeability leads to high voltage induction and ultimately to higher power density of a coil. A coil achieves higher effective permeability when the core allows a lengthy magnetic flux path from the north pole to the south pole.

3.2 Demagnetization Factor

A demagnetizing factor D is geometry-dependent parameter which increases with the increase in the demagnetizing field H_D and decreases with increase in the magnetization *M* of the core where demagnetization field is the resistive tendency to magnetization of a geometry and affect the total magnetic field concentration in the core [13]. The demagnetization field H_D mainly depends upon the geometry of core and can be calculated by equation 2:

$$D = H_D / M \qquad (2)$$

Effective permeability u_{eff} has inverse relation with the Demagnetization factor. As discussed earlier, effective permeability is our prime focus and its dependence on both geometry and material make it an important parameter. So in order to increase the induced voltages, effective permeability needs to be increased and that will happen when demagnetization factor is low. So it can be inferred that core design should be properly addressed. Effective permeability is calculated by:

$$u_{eff} = \frac{u_r}{1+D(u_r-1)} \qquad (3)$$

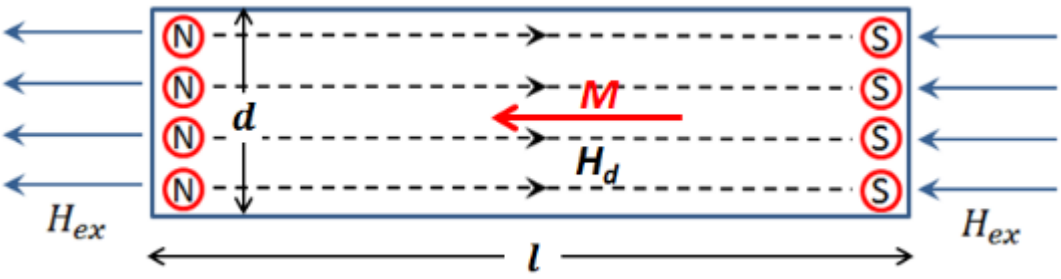

Figure3.1: The demagnetizing field H_D inside a ferromagnetic core when applying external magnetic field H_{ex}

3.3 Equivalent Energy Harvesting Circuit

Every inductive coils show similar characteristics when they are placed under magnetic field of certain frequency. Figure 2 shows the equivalent diagram of inductive energy harvester operating at 50Hz. Induced voltages of coil are function of its properties and the external magnetic field. The total coil resistance is equivalent to core resistance and the

copper winding resistance. According to the maximum power transfer theory, a coil inductance which is a factor that resist the flow of current through coil, is minimized by placing a compensating capacitor and the matched load R_L which should have the value of total coil resistance to ensure that maximum power is transferred.

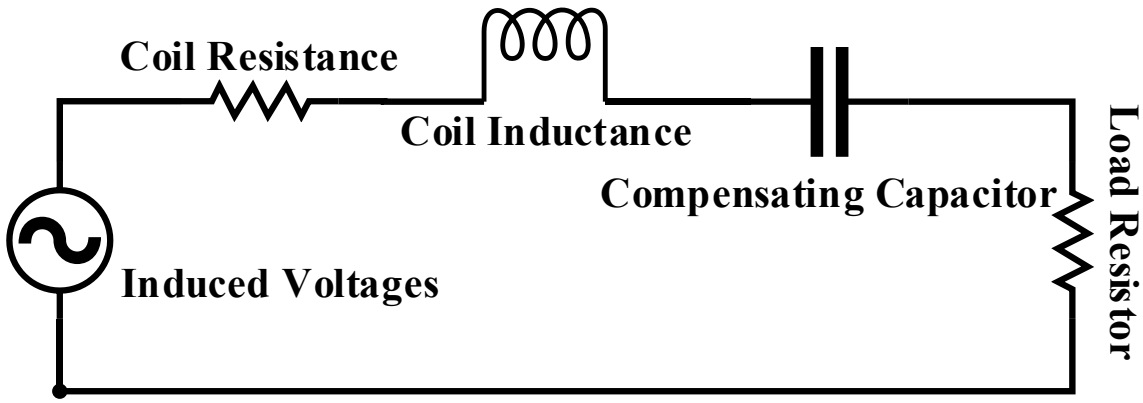

Figure 3.2: Equivalent Energy Harvesting Coil at 50 Hz frequency

Total extracted power at the load resistor is function of induced voltages and the total coil resistance under magnetic field region. is calculated by using equation 4 [12]:

$$P = \left(V_{coil} / 2\right)^2 / R_{coil} \qquad (4)$$

The power density of inductive coil (power output per unit volume), under these attributes, can be calculated from the equation 5 [12]:

$$S_{power} = 0.25 \left(V_{coil}{}^2 / R_{coil}\right) / Vol_{coil} \qquad (5)$$

The equation proposes that power density dependence is not solely upon induced voltages but also on coil resistance under magnetic field and the volume of the coil. V_{coil} is coil's open circuit induced voltage, R_{coil} is the total effective coil resistance when it is placed under the magnetic field region and is the combination of total copper wire resistance that is wound around the core and total core resistance which comes in to play when core is under magnetic field. The values are calculated in ohms. Vol_{coil} is total volume occupied by the coil in m^3.

Since the coil is placed under the power lines for inductive coupling, it is important to understand the flow of electric current in power lines that creates magnetic field in its close vicinity. The frequency of magnetic field in the region of power lines is 50/60Hz depending upon the power system used. Here in Pakistan, the 50Hz power system is used so all the calculations will be dealt under 50Hz frequency. The strength of magnetic field at distance of 1m is in micro-Tesla (10^{-6} Tesla). It is highest at the point of origination and linearly decreases as distance from the originating point increases.

The idea is to initially simulate the different core designs in the ANSYS Maxwell software and by comparative analysis in terms of magnetic field concentration, an optimum design and material will be selected. Using the parameters stated in Faraday's law and demagnetization factor, a coil will be simulated and designed in the environment of Medium voltage power lines (11kV) by Finite Element Method (FEM) in Maxwell which is briefly discussed in the next chapter.

SUMMARY

The chapter includes fundamental concepts that are the basis of the research. Chapter starts with discussing the Faraday's law of induction and briefly describes the parameters that will be focal point during research. It was learnt that effective permeability is an important parameter that needs to be properly investigated and optimized as power density is indirectly linked with it. Effective permeability is further dependent upon demagnetization factor which is a geometry dependent parameter that resist magnetic field concentration and has inverse effect on effective permeability. Chapter concludes with equivalent energy harvesting circuit that describes how every coil shows a similar characteristic when it is placed under magnetic field region.

Chapter #4

FINITE ELEMENT ANALYSIS IN ANSYS MAXWELL

4.1 Introduction:

ANSYS Maxwell is a premier software that uses Finite Element Analysis in order to solve low-frequency Electromagnetic (EM) field problems. It is tasked to design and analyze two-dimensional in XY planes and three-dimensional in XYZ planes EM fields by using finite element method which is a highly precise technique to solve static, frequency-domain and time-varying EM fields [20]. It automatically solves the problems once the material properties and geometrical design is defined. ANSYS Maxwell analyze the design in a finite space region while utilizing the Maxwell equations [21]. The software uses geometry primitive based modeling techniques to have successful operations. Following are the steps needed to be addressed for an accurate simulation in ANSYS Maxwell.

4.1.1 Solution Types

In ANSYS Maxwell, simulations are done under two solution type techniques, Magnetic Solver and Electric Solver. Each solution type has specific task with its own setup and solution method. These solvers solve Maxwell's equations under the extent of particular solution type. Magnetic solver analyze the magnetic field related problems of a model and are further divided into Magnetostatic, Eddy Current and Transient solvers. Similarly, Electric simulator solves Electric potential, Electrical field, current density and electric flux density by using the potential parameter [22]. Since Finite element analysis of our research is dependent upon the Magnetic solvers so only this solver will be our main focus.

4.1.1.1 Magnetostatic

Magnetostatic solver is set by-default when ANSYS Maxwell starts. In this solver, both the object and the magnetic field are in the static state. The sources of static magnetic field include when DC current is passed through conductors, permanent magnets or when external boundary conditions specify the magnetic field as static. The Magnetostatic solver can analyze solenoid, inductor, actuators and motors. The results are in the form of magnetic field (H) from which current density and magnetic field density can be calculated. Following Maxwell equations are solved by the Magnetostatic solver in Maxwell 3D:

$$\nabla \times \vec{H} = \vec{J}$$
$$\nabla \bullet \vec{B} = 0$$
$$\vec{B} = u_o(\vec{H} + \vec{M}) = u_o \cdot u_r \cdot \vec{H} + u_o \cdot \vec{M}_p$$

4.1.1.2 Eddy Current Analysis

On selecting the eddy current solution type, eddy current analysis can be performed. Analysis are applicable to the inductors, solenoids and motors. They can be analyzed in steady-state and time-varying magnetic fields in frequency domain. Both objects to-be analyzed and sources are kept in steady state Like Magnetostatic, eddy current extract results in Magnetic field which can further calculate the Magnetic flux density (B) and Current density (J).

4.1.1.3 Transient Magnetic Analysis

Transient magnetic solution type allows to perform Transient magnetic analysis that has applications in solenoids, inductors, motors and actuators. It performs analysis and computes the magnetic field in the time-domain. Static magnetic field is formed either by time-varying current in conductors or by permanent magnets. Similar to other Magnetostatic solvers, it also computes magnetic field which further allows to calculate current density (J) and magnetic flux density (B). The finite element analysis of our research is also done in transient mode where voltage and current excitations were given

to windings. Transient magnetic solution type gives advantage of connecting external circuit with the windings that allows to define accurate definitions to the designs.

4.1.2 Material Selection

ANSYS Maxwell library occupies a large range of materials that can be assigned to models and designs. Since finite element analysis for our research were done in the transient magnetic mode so the parameters of material will be relevant to transient analysis. In transient analysis, the following parameters can be defined to an element:

4.1.2.1 Relative Permeability:

In magnetic field solution, relative permeability is an important parameter. Relative permeability is the property of the material that determines the allowance of magnetic field lines from inside the material. Higher the material's relative permeability corresponds to better magnetic flux concentration inside material.

4.1.2.2 Core-loss Type:

The core-loss is the combination of eddy current losses and hysteresis losses in a transient solution type. For applications in electrical machines or core transformers where electrical steel or other ferromagnetic materials are used, core losses selection in ANSYS Maxwell give the ground and realistic results.

4.1.3 Boundary Conditions

When a model is designed, ANSYS Maxwell automatically generates the vacuum region which can be edited by the user according to the need. At the interfaces or edge of region, the behavior of magnetic field is defined by boundary conditions. When no boundary conditions are defined for surface, Maxwell generates two type of boundary conditions, first is natural which is the boundary interface between two objects where magnetic field is passed through between objects without any interruption and second is Neumann which is for exterior boundaries [23]. Unlike natural, magnetic flux cannot cross the boundary. Boundary conditions is further divided into three types:

i. Zero Tangential H-Field
ii. Tangential H-Field

iii. Insulating

4.1.4 Meshing

Meshing is an optional operation that allows to refine settings of the model, in ANSYS Maxwell, that are very critical to performance of model under Electromagnetic field. When model's meshing guidance is provided before the analysis, the number of passes to converge a field solution are reduced and field behavior is found even when only few passes are solved making the analysis and convergence faster [23].

4.1.5 Excitation

In transient solvers, the coil parameters such as coil resistance, number of turns and parallel path are needed beforehand. Solver also needs to provide information about the type of excitation that how coil will be connected to sources like voltage, current or external circuit [24].

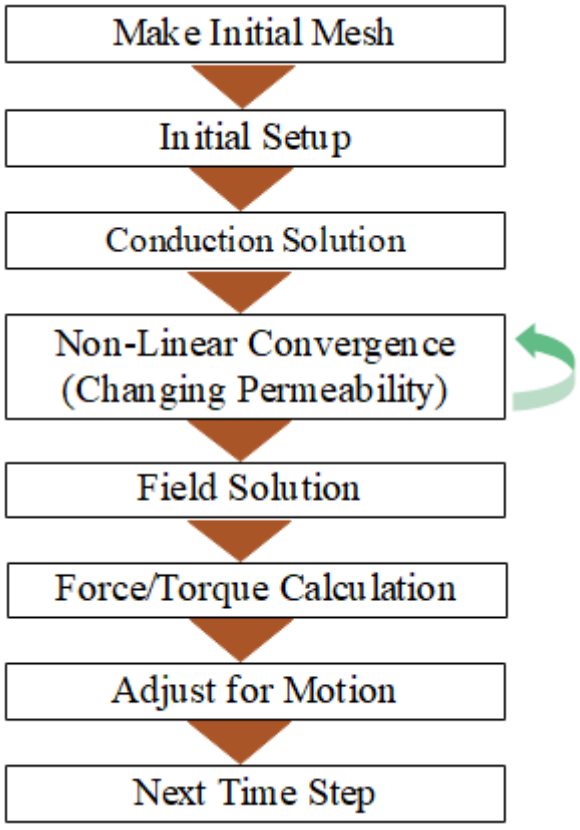

Figure 4.1 Transient Analysis Solution Process in ANSYS Maxwell [25]

4.1.6 Solution Process

Once the conditions of the pre-processing are well defined, an automated solution process takes over and step-through following steps.

4.2 Finite Element Analysis

Since our application lies under the time-varying magnetic field mode, so the environment of transient solver was selected for the optimization of the core material and design. The air region was selected for FEA for realistic results.

4.2.1 Three-Phase Conductors:

The first step was to create 3-phase conductors which are the source of magnetic field region. The standard material for the 11kV 3-phase conductor is Aluminum which was set while designing. After defining the standard parameters, they were excited by current with the following equation:

$$I = \sqrt{2} I_{rms} Sin\left(\omega t \alpha\right)$$

where I_{rms} is the current variable passing through conductors of 11kV lines, ω is angular velocity which is equal to 2πf and α is defined in degrees ±120. The Phase1, Phase2 and Phase 3 would be put in equations as +120, -120 and 0 degrees, respectively. Standard I_{rms} value is 240A which was set while defining variables. Table 4.1 shows the dimensions for making 3-Phase conductors.

Dimensions (mm)	**Phase I**	**Phase II**	**Phase III**
Center Position	850,0,-1250	0,0,-1250	-850,0,-1250
Radius	50	50	50
Height (Length)	2500	2500	2500
Excitation	Current	Current	Current

Table 4.1: Parameters for 3-Phase Conductors in ANSYS Maxwell

A region of magnetic field was created after simulation and the results verified the study [26]. Magnetic field strength was highest at the originating points of the conductors and

decayed as the distance was increased from them. At the distance of 1 meter, 5-10uT of magnetic field density was observed.

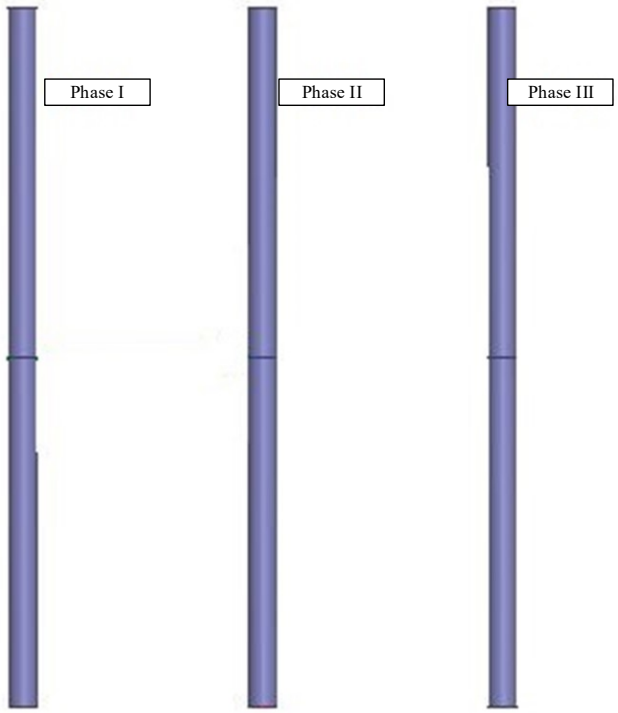

Figure 4.2: Top-View of 3-Phase 11kV conductors in ANSYS Maxwell

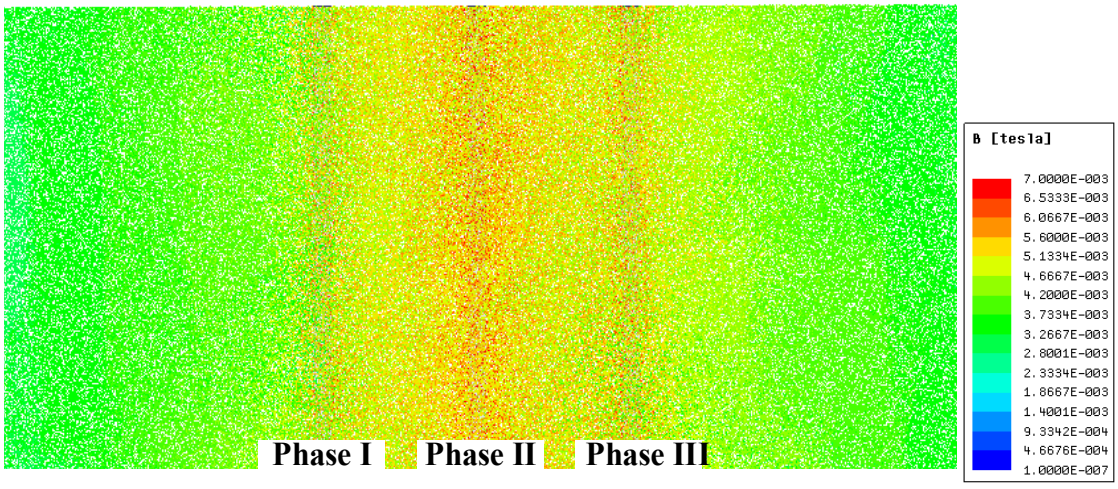

Figure 4.3: Top view of Magnetic field around 11kV at 0.01s

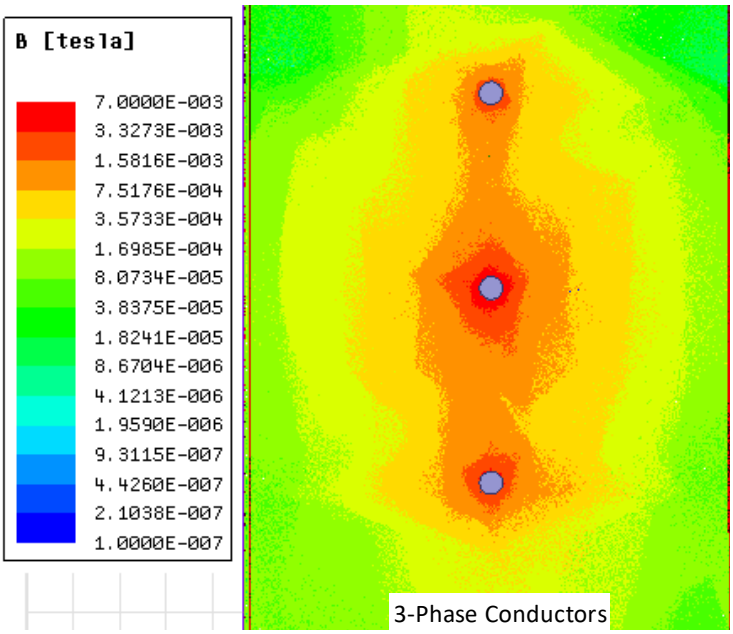

Figure 4.4: Side view of Magnetic field around 3-Phase 11kV at 0.01s

4.2.2 Core Materials and Geometries

Finite Element Analysis will be done on the basis of comparative analysis using certain geometries while providing them different materialistic characteristics. ANSYS Maxwell has vast library of ferromagnetic materials but for comparative analysis, three materials such as Ferrite, Silicon-Steel and Mu-Metal will be provided to geometries. Silicon steel was not available in software so it was added externally. Table 4.2 provides the relative permeability (u_r) of ferromagnetic materials available in ANSYS Maxwell.

Ferromagnetic Materials	**Relative Permeability u_r**
Ferrite	2000
Silicon-Steel	2000-20000
Mu-Metal	60000-100000
Iron	4000
Cobalt	250
Nickel	600

Table 4.2: Relative Permeability of Ferromagnetic Materials in ANSYS Maxwell

After consideration and defining the ferromagnetic materials, geometries like Rectangular Sheet Core, Cylindrical Core and Cone-Shaped Core were simulated. Every core geometry was analyzed by setting materials property to Mu-metal, Ferrite and Silicon Steel.

4.2.3 Rectangular Sheets:

The first of geometries was rectangular sheet which were stacked upon each other. Prime motive behind the stacking was to increase the core thickness It is already said that increasing the core thickness lead towards better magnetic flux concentration. Stacking method is taken from the transformer where sheets are stacked upon each other for better magnetic flux linkage. Core was placed at the distance of 1meter from the 3-phase conductors and every coil was analyzed at this distance for fair comparative analysis. The parameters of single rectangular sheet are described in table 4.3. Rectangular coil was externally connected with the circuit made in ANSYS Maxwell Circuit Editor. External circuit diagram is shown in figure 4.5.

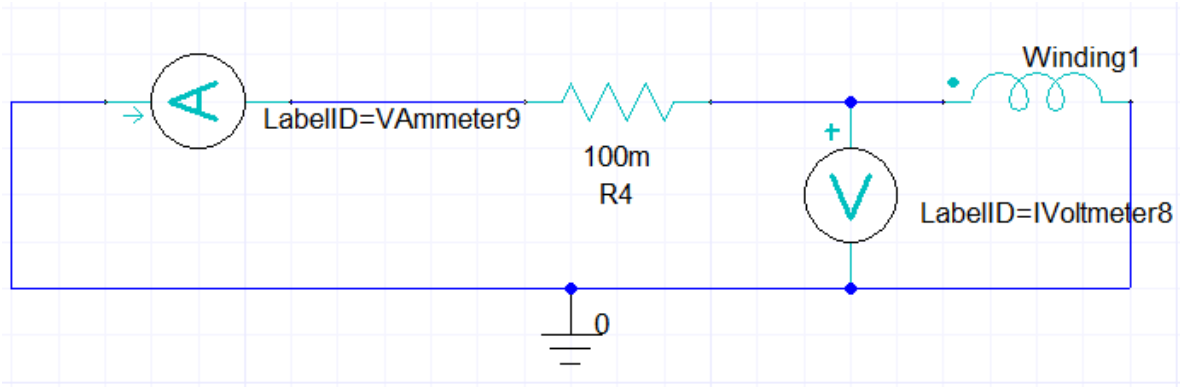

Figure 4.5: External Coil excitation in ANSYS Maxwell Circuit

Parameters	**Values**
Length of Rectangular Core	80mm
Width of core	20mm
Core thickness	0.25mm
Total core thickness (10sheets stacked)	2.5mm
Number of turns	1000

Table 4.3: Rectangular Core sheet parameters

Figure 4.6 illustrates the magnetic field concentration inside the rectangular sheet core. 3D-design of rectangular stacked sheet is shown on the left. On comparing magnetic field concentration in three core materials, it is seen that Mu-Metal sheet permeabilize more number of magnetic field lines than Silicon-Steel core and Ferrite. Although, effective area of Mu-Metal and silicon steel looks similar but more red-spots shows the intensity of magnetic field lines in Mu-Metal sheets are greater than silicon steel core. The intensity of the magnetic field is high at the center as concentration level goes upto 10^{-3} Tesla and lower at the corner of sheets. Ferrite on the other hand did not show well with intensity of magnetic concentration and low effective area among other two materials. This result proved the concept that relative permeability is an important parameter and should be considered seriously while designing coil. As it is already been said that relative permeability increase the effective permeability which ultimately cause more induced voltages.

4.2.4 Cylindrical Core

Cylindrical core is very common in the field of inductive coupling so it was decided to analyze by FEA in ANSYS Maxwell. The circumstance under which it was designed and simulated were same as rectangular sheets. Length of cylindrical coil was set to 150mm and radius was 50mm. It was placed at the distance of 1meter. Core was excited by current in ANSYS Maxwell circuit editor.

Figure 4.7 illustrates that magnetic field concentration in the cylindrical core is better than rectangular sheets as the number of magnetic field of lines that are passing through the cylindrical core are higher. The effective area under the external magnetic field is larger which infers the result that demagnetization factor of cylindrical core is low that cause magnetic field of lines to lengthen their path inside the core. Mu-Metal cylindrical core shows red-spots which is suggesting that in that particular area magnetic flux is higher. Effective area and intensity of magnetic field lines are better in Mu-Metal than Silicon-Steel and ferrite which further proves the relative permeability's inverse relation to the demagnetization factor.

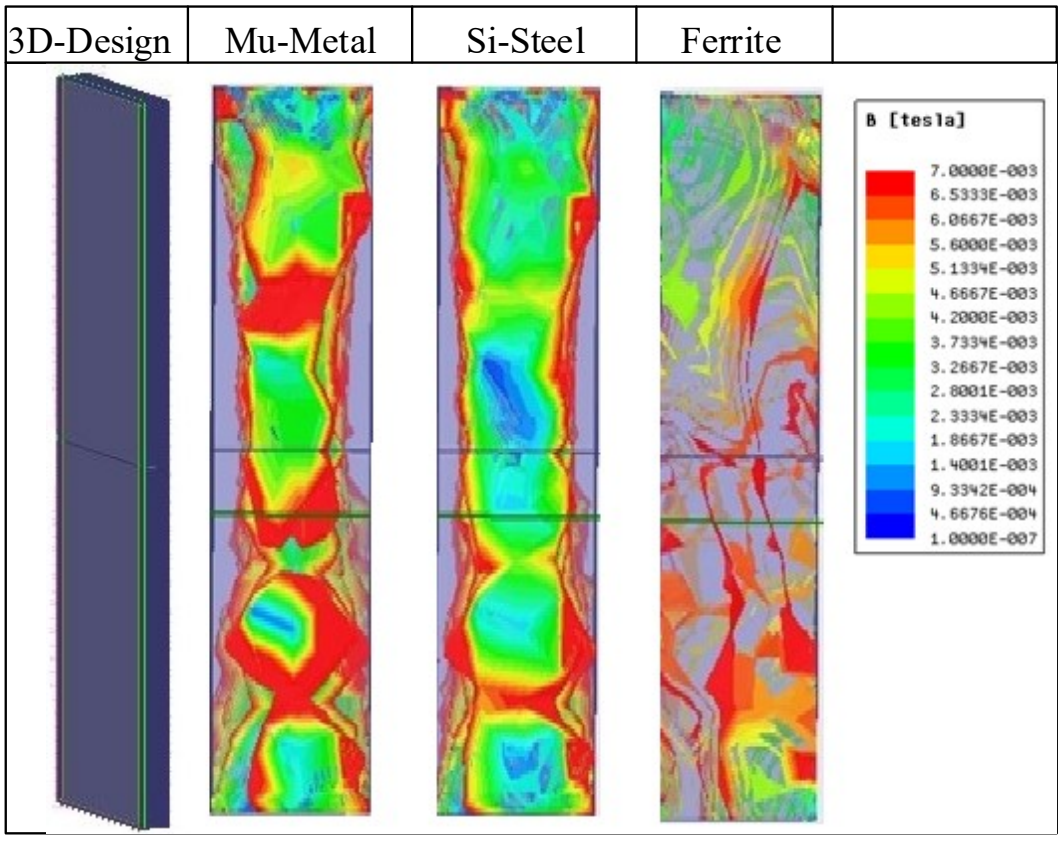

Figure 4.6: Graphic illustration of Magnetic field concentration in Rectangular Sheets

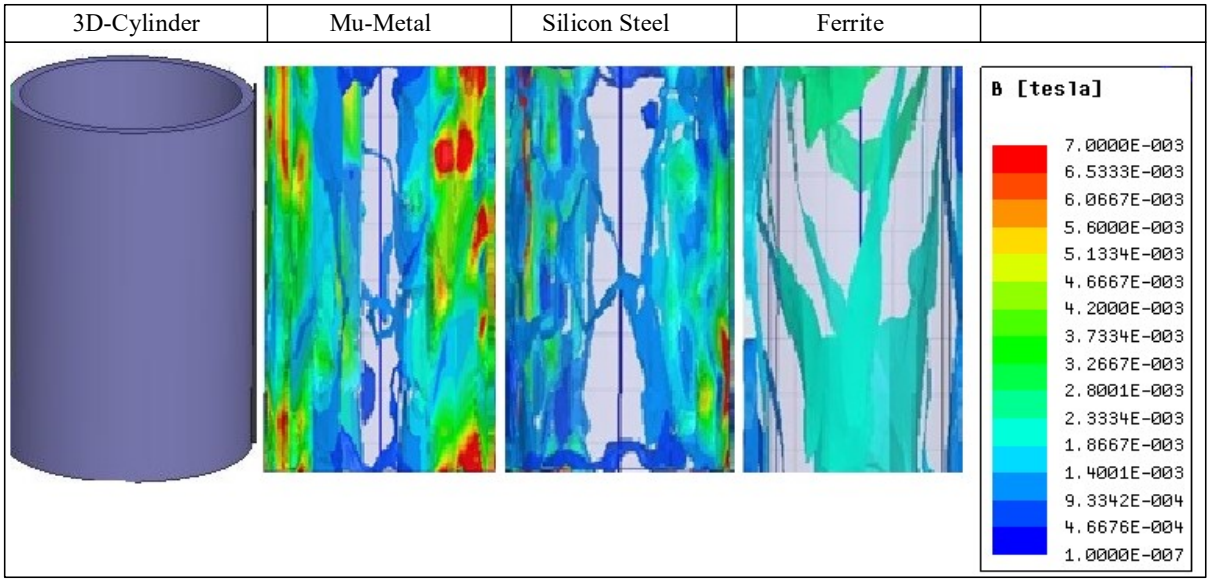

Figure 4.7: Graphic illustration of Magnetic field concentration in Cylindrical Core

4.2.5 Cone-Shaped Core:

The last of simulated design was Cone-Shaped design which is used in Microelectromechanical system (MEMS) for magnetic field concentration purposes. Cone-shaped core was simulated under the similar environment as previous designs. Core was made with the parameters shown in table 4.4.

Parameters	**Values**
Length	150mm
Upper Radius	20mm
Lower Radius	40mm
Distance from 3-Phase conductors	1000mm
Number of turns	1000

Table 4.4: Parameters of Cone-Shaped Core

Figure 4.8 illustrates the response of cone-shaped core with different materials under the magnetic field region created by 11kv power lines. Visual representation of cone-core shows that Mu-Metal has more effective area under magnetic field than Silicon Steel and Ferrite. Magnetic field is intense and dense in Mu-Metal. Red-spots, which shows number of magnetic field lines intensity, are more in Mu-Metal.

On comparing with other designs, Magnetic field concentration in the highest in Mu-Metal cone shaped core. Mu-Metal cone coil had the lowest demagnetization factor which allowed larger magnetic field to pass through the design. The magnetic flux inside the cone-coil was visualized in order of 3-7mT. It was also realized that magnetic flux concentration was maximum at the center and lower at the both ends.

4.2.6 Average Magnetic Flux

Using field calculator, average magnetic field passing through the design can be calculated and exact number can be found. Table 4.5 also verifies the results obtained by visualization. On comparison of all three designs and materials, it can be stated that Mu-Metal cone should be used for making inductive coil.

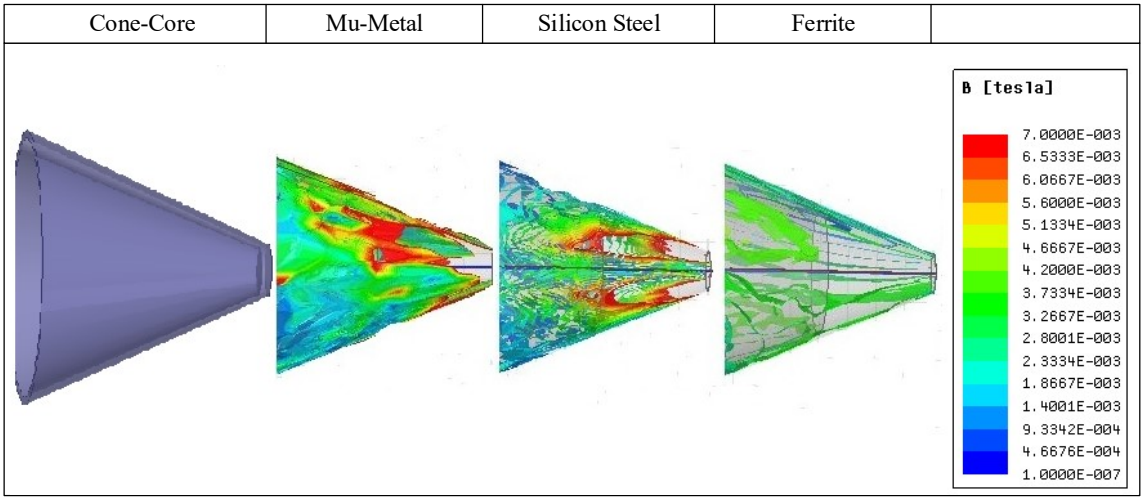

Figure 4.8: Graphic illustration of Magnetic field concentration in Cone-Shaped Core

Ferromagnetic Materials	Cone-Core	Cylindrical Core	Rectangular Core
Mu-Metal	0.0032	0.0027	0.0021
Silicon Steel	0.0028	0.002	0.0019
Ferrite	0.0021	0.0015	0.0015

Table 4.5: Average magnetic flux in Simulated Cores in Tesla (T)

SUMMARY

Chapter starts with the introduction of ANSYS Maxwell which was used for the Finite Element Analysis. Important parameters that were part of the FEA of the design, were discussed in detail. Afterwards, 11kV 3-phase environment was analyzed under which all the simulation had to be done. A section in this chapter was reserved for different ferromagnetic materials that will be used with core geometries. The ferromagnetic materials like Mu-Metal, Silicon-Steel and Ferrite were simulated with the geometries like rectangular sheets, cylindrical cone and cone-shape cores. FEA showed that Mu-metal cone-shaped core has very good magnetic field concentration and it can be used for the inductive coupled coil.

CHAPTER#05

PHYSICAL COIL DESIGNING

Before designing the coil, it is important to get knowledge about the components that will be used while designing the coil. Conventional inductive coil is made up of a ferromagnetic core material of a certain shape and a copper wire that is wound on core to make up a coil. Results in Finite Element Analysis showed that Mu-Metal is better ferromagnetic material among its other counterparts and when the core material is given cone shape, the results of magnetic field concentration goes even better. So, this chapter starts with a brief overview about the materialistic and physical properties of Mu-Metal which will help us designing and making the coil.

5.1 Mu-Metal

Mu-Metal is a very high permeable soft ferromagnetic alloy of Nickel and Iron. It comes with several compositions such as 77% nickel, 16% iron, 5% copper, and 2% chromium or molybdenum and composition of 80% Nickel and 20% iron [27-28]. Conventionally, Mu-Metal has been used for shielding very sensitive electronic equipment against DC and AC fields. The typical relative permeability values of Mu-Metal lie around 60000-300000 which is several thousand higher than ordinary steel or silicon-steel. Mu-Metal is a soft ferromagnetic material which allows it to mold it into any shape relevant to compatible applications. Another advantage with Mu-Metal over similar permeable materials is its ductility and workability that allows to be easily formed into very thin sheets for shielding purposes. The only concern with Mu-Metal is low magnetic anisotropy (ability of a ferromagnetic material to resist demagnetization when it is placed in external magnetic field) and magnetostriction (property of ferromagnetic material to expand or contract when exposed to magnetic field region) giving it a low coercivity so that it saturates at low magnetic fields but since our application lies in the range of magnetic field strength of micro-tesla, Mu-Metal can be efficiently and effectively utilized. Mu-Metal has low resistivity in the order of 10Ω which in comparison to ideal material should be very high of order $10^{10}\Omega$. Another reason to choose Mu-Metal despite having low resistivity of

60μΩcm and low saturation of 8000Gauss, as compared to Silicon steel which has high saturation level of 22000 Gauss, is availability of very low magnetic field density under MVTLs and HVTLs, in uT with 50/60Hz frequency. For our application, the high relative permeability of Mu-Metal is needed which will permeabilize more number of magnetic field lines.

5.2 Mu-Metal Cone-Core

For research purpose, 6 Mu-Metal sheets were bought by MAGNETIC SHIELD CORP. with 0.010" thickness and 8" x 12" of length and breadth respectively. These flat Mu-Metal sheets are moldable so they were cut and given the cone-shape. Figure 5.1 shows the Mu-Metal sheet that is molded into a cone shape and that will be used as a core for inductive coupling coil.

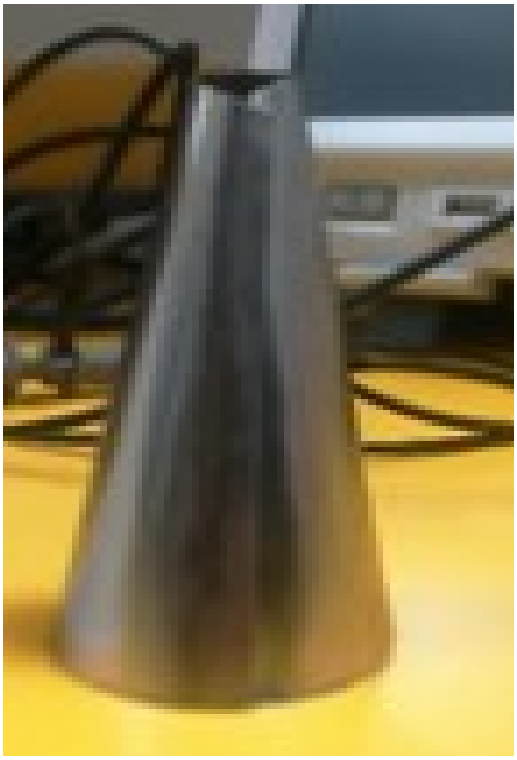

Figure 5.1 Mu-Metal Cone-Core

It should be notified that induced voltages have direct relation with core air-gaps because air gaps allow the increment in demagnetization factor which ultimately cause reduction in magnetic flux-linkage with the inductive coil. This reduced flux-linkage further cause reduction in voltages induction. In simulation, a perfect cylindrical and truncated-cone

were simulated which were free of any air gaps but in practical, it is difficult to make cone shape cores from metal sheets without air gaps. The cone-core showed above has core-gaps but it was kept as minimum as possible to have good results. A singular cone-core were given the following dimensions:

Parameters	**Values**
Length	130mm
Upper Radius	20mm
Lower Radius	40mm
Air-gap	1mm

Table 5.1 Physical design of Cone-Core

5.3 3D-Printed Cone

Mu-Metal sheet is a very slippery material and cone-shape makes it more difficult to do copper winding on it. As a results, a cone was designed in Ultimaker software, which designs 3D object for printing, and printed from 3D printer. Mu-Metal cone sheets were placed upon this printed cone to give stability while winding of copper wire on cone-shaped Mu-Metal layers. Figure 5.2 shows the printed 3D-cone.

Figure 5.2: Printed 3D-Cone

5.4 Copper Wire:

SWG-32 enameled copper wire was chosen for winding around the core which had diameter of 0.274mm and resistivity of 0.292 Ω/m. The selected enameled wire was smaller in diameter as it gave more turns on fixed core volume which ultimately caused to induced more voltages. Core material has its own resistance when it is placed in the magnetic field which resist the induced voltages so in order to have low resistance an optimum copper wire should be selected that does not occupy large area and gives more turns. The wire resistance was 225Ω at 4000 copper turns. Wire resistance was calculated by Multi-Meter. Since core resistance does not account until it is placed under the magnetic field region, it is desirable for coil resistance to be equal to wire resistance. This makes core resistance to be negligible which is tried to make sure during designing the cone-coil. Another important parameter while choosing a copper wire for winding is that it can deliver the maximum power whereas also keeping the resistance of coil as minimum as possible because enameled wire directly affects the coil resistance, voltages, power and power density. Figure 5.3 gives the illustration of cone-core coil.

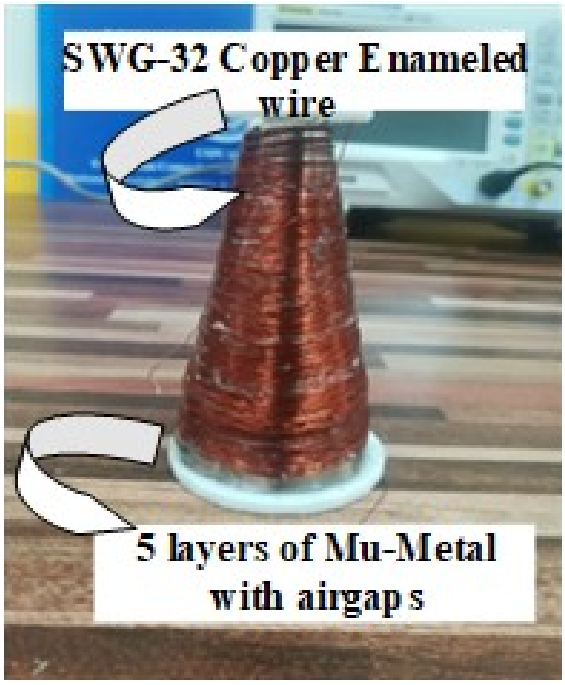

Figure 5.3 Final Cone-Shaped Core Coil

5.5 Helmholtz Coil

Before testing the coil under the overhead power lines, it was feasible to test the coil in Laboratory. To create an environment like 11kV power lines where magnetic field is present, a coil was designed. Helmholtz coil consists of two identical circular coils that generates the nearly uniform magnetic field. It consists of twin circular magnetic coils which are separated by distance equal to the radius of the coil. Magnetic field density of Helmholtz coil can be calculated by the following formula:

$$B_{Helmholtz} = \left(0.8\right)^{3/2} \mu_o NI / R_H$$

where μ_0 is the vacuum permeability, N is the number of turns, I is the current passing through the coil and R_H is the radius of the Helmholtz coil. Equation suggests that for a strong magnetic field density, Helmholtz coil should have high current and higher number of turns. For our experimental purpose, a Helmholtz coil was made with 300 copper turns on each coil with 5.5mA of current was passed through upon excitation by Waveform generator at 50Hz frequency. The radius of each coil was 100mm and were separated by same distance as of radius. Coil was able to produce a maximum magnetic field density of 15uT at the center.

Figure 5.4: Helmholtz Coil with Cone-Coil in middle

SUMMARY

Chapter 5 starts with the section mentioning materialistic and physical properties of Mu-metal that is to be used for the inductive coil. It is briefed that Mu-Metal has very high relative permeability, high ductility and ability to mold into any geometry of interest. The chapter goes on showing that how Mu-Metal sheets was molded into cone-shape. A 3D-printed design is briefly mentioned that why and how it gives stability and easiness while making the coil. Chapter concludes with the discussion of enameled copper wire SWG-32 that how it affects the parameters like induced voltages, power and power density.

Chapter#6

COIL EXPERIMENTATION

After brief description of coil designing and its parameters, this chapter will discuss the experimentation done by the cone-shaped coil by exposing it to the external magnetic field.

6.1 Open-Circuit Configuration:

Helmholtz coil was powered up by the Waveform generator at the frequency of 50Hz. Since 11kV produces 15uT at the distance of 1m, a spot was found by Magnetic field-meter where strength of magnetic field was 15uT. It is worth to mention that a single-core coil was initially placed under magnetic field region. Number of turns were gradually increased. Table I provides the induced voltage of single mu-metal cone coil on increasing the copper turns.

N (Number of turns)	**Vin (Voltages Induced)**
240	35mV
480	65mV
1200	130mV
2400	250mV
3000	300mV

Table 6.1: Induced voltages when single-layered Mu-Meta coil was placed under 15uT magnetic field

A linear trend can be seen that on every 240 turns the induced voltages almost gets doubled. Under this scenario, the induced voltages were low so number of Mu-metal layers were gradually increased. Since thick core tends to have higher induced voltages, number of layers were increased to 2,3,4 and 5 which in response induced 420mV, 590mV, 770mV, and 1V respectively at 3000 turns under 15uT magnetic field as shown in Table 6.2. This proves the concept that on increasing the core width, there is more concentration of magnetic flux, lesser demagnetization factor and more flux linkage

which ultimately gives the results in better voltage induction. Number of copper turns were kept to 3000 turns for testing of coil.

Mu-Metal Layers (n)	Induced Voltages
2	420mV
3	590mV
4	770mV
5	1000mV

Table 6.2: Induced voltages when coil at 3000 copper turns was placed under 15uT magnetic field at different layers

For experiments, the 5-layers of Mu-Metal were used to increase the thickness and to prove the concept. Further increase in the core layers make the coil heavy and expensive which is undesirable. The coil was able to induce voltages of 1.5V when number of copper turns were increased to 3950. It is noteworthy to mention that as copper turns are increased, the total coil resistance is also increased which affects the power and power density. Figure 6.1 illustrates the open-circuit configuration (when no load is connected).

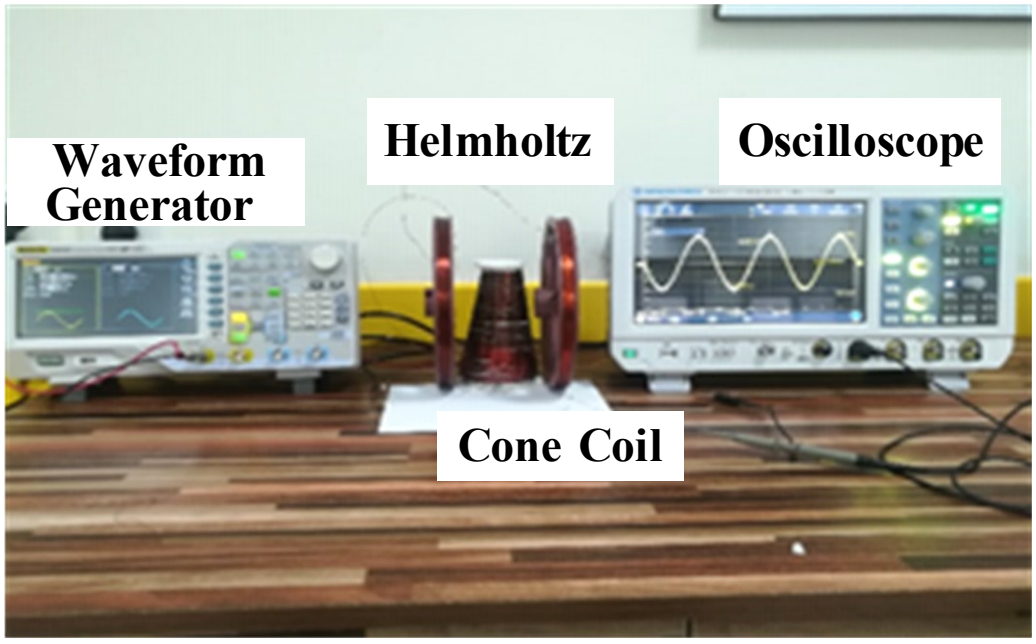

Figure 6.1: Open Circuit Configuration of Cone-Coil

For calculation of the results, Multi-meter and Oscilloscope was used. The probes of oscilloscopes can be seen connecting with the output terminals of the coil, in the figure 6.1.

Figure 6.2 describes the relationship between the copper turns on Mu-metal cone-core with the coil resistance. There is a linearity in the graph that on every 450 turns, coil resistance gets double. In the range between 3500-4000 copper turns, there is a slight sharp increase in the coil resistance, that is because that on every copper layers on core, coil thickens and more coverage of wire is needed to complete a single turn. That makes increase in the coil resistance.

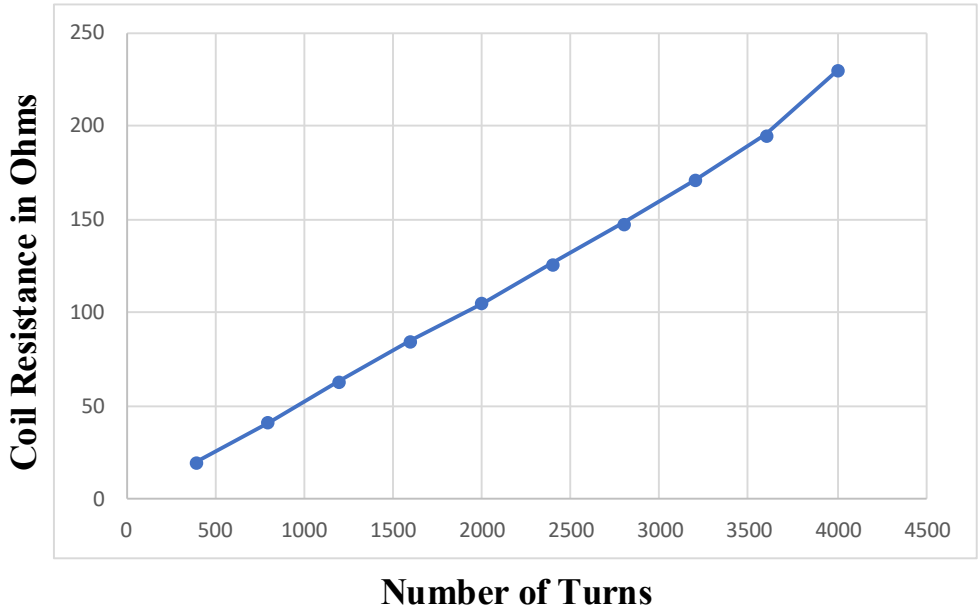

Figure 6.2: The effective coil resistance without placing under magnetic field as function of copper winding

It has already been said that increase in winding turns increase the induced voltages. Figure 6.3 illustrates that trend of voltage induction with the increase of copper turns in cone-coil. Linearity was observed in relationship between voltage induction and copper turns. At start, the voltage induction is low but as the copper layer is increased, the process of induced voltages also increases. The graph proves the Faraday's law of induction that there is linear increase in V_{in} on increasing N.

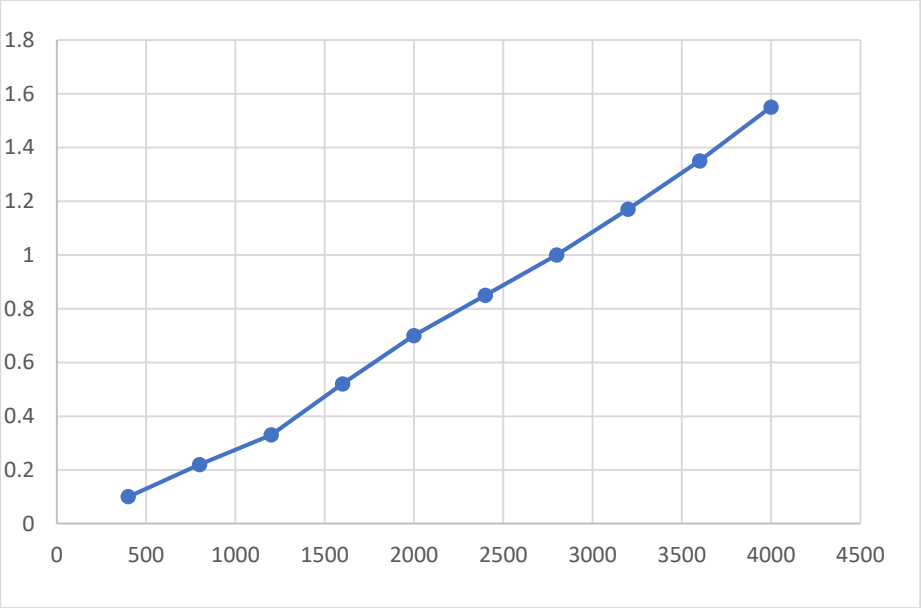

Figure 6.3: The 5-layered Cone-coil induced voltages as function of winding numbers

6.2 Closed-Current Configuration

6.2.1 Energy Harvesting Circuit

EHC is made to convert and control induced voltage from inductive coil in a form that is compatible to our application. Since components of circuits consume energy and energy harvested from coil is not very high, it is important to make circuit that is enough efficient to consume energy that is smaller than harvested energy. EHC should also be able to ensure to meet power requirement of desired application.

6.2.1.1 Multiplier Circuit

Voltage Multiplier Circuit delivers output of multiplier DC voltages on applying the low Input AC voltages. It is made up of capacitors and diodes. Since the output voltages need to be in pure DC form to function the end device i.e. sensor nodes, induced voltages which are in AC form, were to be rectified in DC voltages.

Multiplier circuit works on two cycles, Positive Half-Cycle and Negative Half-Cycle. During the positive half cycle, Diode D_1 becomes forward biased, making it to conduct current. Current flows to the capacitor C_1 and charges it to positive peak value of input voltage. During the positive Half-cycle current does not flow through capacitor C_2

because the diode D_2 becomes reverse biased. So the diode D_2 blocks the current flow towards the capacitor C_2. Therefore, during the positive half cycle, capacitor C_1 is charged whereas capacitor C_2 remains uncharged.

During the negative half-cycle, things work in the opposite manner as D_1 goes reverse biased, which makes it to block the current and hence C_1 does not charge. Charge stored in C_1 start discharging. On the other hand, D_2 starts working after becoming forward biased and C_2 gets fully charged. The voltages of discharged C_1 and input voltages are added to C_2 which takes the total value to $2V_{in}$. On connecting the load with C_2, voltages discharge from capacitor and goes to load.

In our work, the coil was connected with a Cockroft-Walton multiplier circuit that functioned like a rectifier circuit. We used a half-wave voltage doubler circuit that was consisted of two-diodes and two-capacitors connected to an Input AC voltages which are induced by inductive coil. While converting AC voltages to DC, it also boosted up the rectified voltages according to the number of stages of multiplier circuit. Here a double-stage multiplier circuit was used that added the peak-to-peak voltages. Since normal Germanium and Silicon diodes drop the voltages from 0.3V to 0.7V respectively, it was totally undesirable to utilize the conventional diodes in multiplier circuit. Instead, Schottky diodes of model PMEG1020EA were used that had voltage drop of 0.1V. Two capacitors of 6.8mF were used with these diodes for the construction of Multiplier circuit [16].

6.2.1.2 Buffer Circuit

A buffer circuit is a circuit that isolates one circuit from another one. It makes sure that voltages from multiplier circuit is provided to DC-DC converter when storage capacitor is fully charged and cut off the supply from coil to DC-DC converter, once the sufficient voltages were not supplied by coil to charge the storage capacitor, which happens specifically when there is insignificant magnetic flux linkage to the coil.

The buffer circuit was formed by LT1034, current comparator LT1017 and MOSFET switches as proposed in the research [11]. The internal circuit diagram of LT1034 is shown which consists of 100kΩ, 1MΩ, 680kΩ and one zener diode 1N2804. It is a voltage

reference IC that produces fixed voltages. In our circuit, zener diode makes sure that excess energy is safely dissipated whenever coil is exposed to higher magnetic field region which ultimately cause higher induced voltages. LT1034 is further connected to current comparator IC LT1017 which compares the current coming from the multiplier circuit and LT1034, if the current is larger than the certain number, it releases output in terms of voltages. Figure 6.4 shows the circuit diagram of Energy harvesting circuit that shows the induced voltages connection with highlighted Multiplier circuit and Buffer-Circuit.

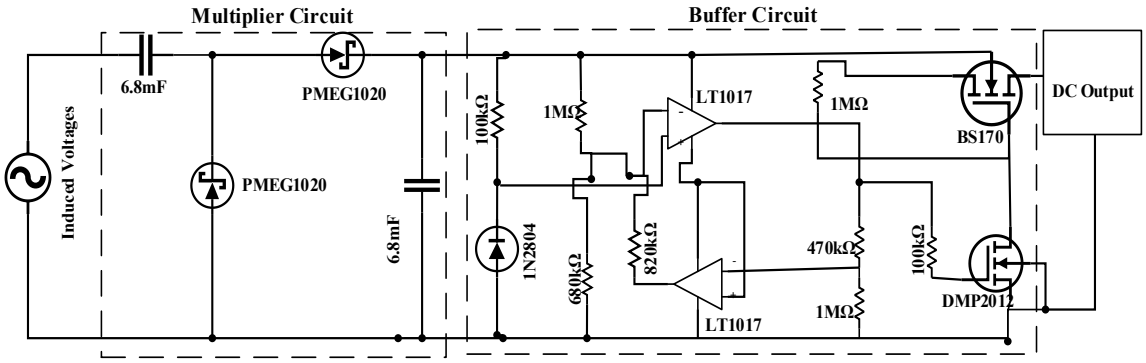

Figure 6.4: Energy Harvesting Circuit

The DC output voltages can be further connected to DC-DC converter for further boosting up the voltages according to the application of wireless sensors. In our research, the circuit was terminated at the Buffer circuit.

At the end of circuit, a multiplied DC output voltages were obtained. Multiplied output DC voltages were actually input peak voltages minus the voltage drop across diodes, which in the case of this circuit was of 1V DC ultimately. Multiplier circuit was further connected to the buffer circuit. Some voltages were consumed in powering up the buffer circuit which ultimately gave an ultimate output of 650mV of DC voltages when capacitors were fully charged.

DC voltages from buffer circuit may be further connected to DC-DC converter if amplified voltages are needed at the expense of current or can be step-down while increasing the current, it all depends upon the application upon which it will be used. The end products are usually low-power sensor nodes that can be directly powered up or batteries that are recharged.

SUMMARY

This chapter described the experimental set-up of our design where inductive coil was placed under the magnetic field region created by Helmholtz coil. Two configurations, Open-Circuit and Closed-Circuit were discussed in detail. In open-circuit configuration, there was no-load connected with the coil and the results came in the form of AC voltages. Both increase in Mu-Metal layers and copper turns led towards significant increase in voltage induction. In closed-circuit configuration, a matched-load was connected at the end of the harvester circuit. An improved EHC was introduced with minimal voltage drops and energy dissipation. Brief comments on EHC and its sections, Half-wave multiplier circuit, Buffer circuit and DC-DC converter were part of the chapter.

Chapter#07

RESULTS AND DISCUSSIONS

The main consideration of investigation was to improve the effective permeability which is the main parameter of Faraday's law. Effective permeability u_{eff} was improved by Finite Element Analysis of various designs with ferromagnetic materials in ANSYS Maxwell. The results led us towards was achieved by designing the cone-coil. The Mu-metal cone-shaped core coil was able to harvest energy from magnetic field. It also proved the concept of Faraday's law of induction. During physical design, it was kept in consideration that volume of inductive coil should be kept comparative to the previous designs so that comparative analysis gets easy.

In previous chapters, we came by discussing simulations, physical designs and experimentations. These chapters directly or indirectly were dependent upon each other. This section is the ultimate result of all the previous discussions. This chapter includes what we achieved by numbers and analyze our numerical results with the previous studies.

7.1 Harvested Power:

By using the equation mentioned below, the total harvester power by the inductive coil, when placed at the magnetic field region, was calculated.

$$P = \left(V_{coil} / 2\right)^2 / R_{coil}$$

Cone-Coil induced 1.4V against the total matched-coil resistance coil transmitted the power of 4.34mW which is enough to power a small wireless sensor [29]. A normal GPRS data logger consumes 3.6W of power [30]. If the data is collected every 15 minutes and the data logger takes a maximum of 1 minute to transmit the information to the server, the average power consumption would be 100 mW. So it can be inferred that proposed design is able to power the conventional sensor nodes.

7.2 Power Density

Cone-Coil shaped achieved total power density of 5.5uW/cm^3 at the magnetic field region of 15uT when the matched-load was connected to the coil. The total volume of the truncated-cone coil was 380cm^3. Power density was calculated by the following formulae:

$$S_{power} = 0.25 \left({V_{coil}}^2 / R_{coil} \right) / Vol_{coil}$$

Although, the power density is low as compared to other conventional energy harvesting techniques like solar and wind but among contactless inductive coupling method, it achieved the better number. Power and power density can be further increased if we increase the total volume of the coil, increase the number of Mu-Metal layers and copper turns and place it in a stronger magnetic field region.

7.3 Comparative Analysis

Table 4 gives a detailed comparison of coil parameters of Cone-Coil with previous studies and method. The proposed cone-coil occupies less space than Solenoid Coil and Bow-Tie Coil. Cone-coil is also simpler in design and easy-to make as only Mu-Metal sheets has to mold into cone-shape. The total wire resistance was 215Ω but when placed under magnetic field region, the total measured coil resistance decreased to 90ohms which on comparison with Solenoid coil is very less. Total helical coil resistance would have been higher than Cone-shaped if copper turns of helical coil would be increased. In terms of power density, our proposed-coil outcome previous contactless inductive coupling methods and had almost twice the power density of Helical coil method. Most of the previous studies were done under the 60Hz frequency power systems. Whereas, we achieved the better results under the 50Hz frequency as according to Faraday's Law, higher frequency leads towards higher voltage induction.

Voltage induction would have been much better if core layers were without air-gaps. The air-gaps led towards less magnetic flux linkage. Proper machine winding of copper wire on core would have made positive impact on induced voltages since manual winding caused improper and misaligned coverage on core. Results can be improved if these parameters are accounted properly while designing the coil.

Coil Parameters	**Helical Coil [14]**	**Solenoid Coil [7]**	**Proposed Cone-Coil**	**Bow-Tie Coil [12]**
Length	15cm	50cm	13cm	15cm
Magnetic Flux	7uT	18.5uT	15uT	7uT
No. of Turns	400	40000	3950	9500
Wire Diameter	0.4mm	N/A	0.274mm	0.14mm
Voltages Induced	185mV	10.5V	1.4V	0.73
Coil Resistance	13.96Ω	33kΩ	90Ω	160.2Ω
Coil Volume	292cm^3	981cm^3	450cm^3	800cm^3
Coil Power	612uW	833uW	4.34mW	0.831mW
Power Density	2.1uW/cm^3	0.85uW/cm^3	5.5uW/cm^3	1.86uW/cm^3

Table 7.1 Comparative Analysis of Coil Parameters of Different Design Methods

If the number of Mu-Metal layers and length of coil are increased, there will be more path for magnetic flux and coverage for copper wire. At the length of 20cm, 7 Mu-metal layers and 10000 turns, it is predicted that induced voltages will be increased to 5V and power density to 20uW/cm^3 can be achieved.

SUMMARY

This chapter compiles the results achieved by the experiments conducted on the Cone-Core Inductive Coil. It was observed that the proposed coil had better results in terms of voltage induction, power extraction and power density than previous studies and methods. A brief comparative analysis with other designs was also part of this section where several coil parameters were numerically compared and extracted results from them. Some problems were also identified in this chapter that lead towards reduced flux linkage and it was concluded that if these problems are properly handled, final results can be even better.

Chapter#8

CONCLUSION

8.1 Thesis Summary

The Magnetic Field Energy Harvesting (MFEH) from medium and voltage power lines is an emerging technology that aims at energizing low-power sensor nodes from the magnetic fields in the vicinity of such lines. The development of this technology contributes to the improvement of the electricity grid by powering up the sensor nodes and charging batteries. Consequently, MFEH has become the focus of research in recent decades.

The main challenge with the MFEH is the ability to extract useful amount of energy by avoiding the direct contact with the power lines. Since, in a contactless MFEH system, coupling is weak with the coil, a thorough understanding of magnetic field and inductive coil parameters is needed. In this thesis, the knowledge and understanding from MFEH is applied in order to optimize and improve the inductive coil parameters.

This thesis demonstrates the usage of power line magnetic field so that direct contact with the power lines is avoided. In previous studies, direct contact-transformers have been used which encloses the current carrying conductors to directly couple the magnetic flux. This method is not suitable for the large cross-sectional current carrying conductors. So contactless inductive coil was thoroughly studied and it was found that effective permeability part of Faraday's Law of induction needs to be improved. For optimization of effective permeability, finite element analysis was done in ANSYS Maxwell.

In FEA, an 11kV power system environment was created under which various geometries with certain ferromagnetic materials were simulated and visual and tabular results were provided in terms of magnetic flux concentration. Mu-Metal Cone-Core showed the best results among its other counterparts and was selected for designing the physical coil.

Thesis then introduces the essential components that needs to be understood before utilizing to make an inductive coil. A flat Mu-Metal sheet was molded into cone-shape

and placed upon 3D-printed cone. SWG-32 copper wire was wound around the core. Helmholtz coil was briefly described as it is source of magnetic field region.

Thesis goes forward with the experiment of the proposed inductive coil which is placed under magnetic field region generated by Helmholtz coil. Results are measured with both open-circuit and closed-circuit configuration. The chapter mentions the Energy Harvesting Circuit and its components briefly that converts the induced AC voltages into rectified DC voltages while multiplying them and buffer circuit which controls the switching between induced voltages and DC-DC converter part.

Results section of thesis displayed the outcome of experiments and comparatively analyzed the different coil parameters with previous coil designs and studies. Proposed coil method was able to induce 1.4V and extracted power with matched-load coil resistance of 4.34mW. Despite having low-volume than most of the previous designs, proposed method achieved better power performance. The ultimate power density was 5.5uW/cm^3 which was better than any previous design.

8.2: Future Recommendations

There are many limitations and constraints related to the topic of power line monitoring. The work presented in this thesis proposed an inductive coupling technique which was able to have improved power density in contactless energy harvesting but when it is compared to the other harvesting technique, it is quite low. The need of improved power density is essential and still a lot of work is needed in contactless inductive coupling to increase the magnetic flux linkage with the coil. Geometry design can be further modified by eliminating the constraint of air-gaps and giving proper copper alignment to the core. Material with very high magnetic material can be utilized for the core but since high magnetic materials are expensive so the cost of coil also needs to be strictly looked. Furthermore, coil needs to be efficient, cheaper and easily deployable while designing.

REFRENCES:

[1]. Manohar singh, Dr. B.K Panigrahi, Dr. R. P. Maheshwari, “Transmission Line Fault Detection and Classification”, Proceedings of ICETECT 2011.

[2]. L. Peretto, ‘‘The role of measurements in the smart grid era,’’ IEEE Instrumentation & Measurement Magazine, vol. 13, no. 3, , 2010 pp. 22--25.

[3]. K. Toussaint, N. Pouliot, and S. Montambault, “Transmission line maintenance robots capable of crossing obstacles: State-of-the-art review and challenges ahead” Journal of Field Robotics, 2009 pp. 477.

[4]. V. Raghunathan, A. Kansal, J. Hsu, J. Friedman, and M. Srivastava, “Design considerations for solar energy harvesting wireless embedded systems,” in Proc. 4th Int. Symp. Inf. Process. Sensor Netw., 2005, pp. 457–462

[5]. G.K Ottman, H.F Hofmann, A.C. Bhatt, G.A. Lesieutre, “Adaptive piezoelectric energy harvesting circuit for wireless remote power supply,” IEEE Trans. Power Electronics, Vol. 17, Issue: 5 2002, pp. 669-676

[6]. J. C. Rodriguez, G. Holmes and B. McGrath, “Maximum energy harvesting from medium voltage electric-field energy using power line insulators” Australasian Universities Power Engineering Conference, AUPEC 2014 - Proceedings. 10.1109/AUPEC.2014.6966633.

[7]. R. Moghe et al., “A Scoping Study of Electric and Magnetic Field Energy Harvesting for Wireless Sensor Networks in Power System Applications,” Proc. IEEE Energy Conv. Congr. & Expo., Sept. 2009, pp. 3550–57.

[8]. O. Cetinkaya and O. B. Akan, "Electric-Field Energy Harvesting in Wireless Networks," in IEEE Wireless Communications, vol. 24, no. 2, April 2017 pp. 34-41,.

[9]. R.H. Bhuiyan, R.A. Dougal, M. Ali, “A Miniature Energy Harvesting Device for Wireless Sensors in Electric Power System,” IEEE Sensors Journal, Vol. 10, Issue: 7, 2010, pp. 1249-1258

[10]. C. Preve, “Protection of Electrical Networks,” ISTE Ltd., ISBN 978-1-905209-06-04, 2006

[11]. N. M. Roscoe, M. D. Judd, "Harvesting energy from magnetic fields to power condition monitoring sensors", IEEE Sens. J., vol. 13, no. 6, 2013 pp. 2263-2270,

[12]. S. Yuan, “A High Efficiency Helical Core for Magnetic Field Energy Harvesting”, IEEE Transactions on Power Electronics, Volume 32, Issue:7,2016 pp. 5365-5376

[13]. Yuan, S.; Huang, Y.; Zhou, J.F.; Xu, Q.; Song, C.Y.; Thompson, P. Magnetic field energy harvesting under overhead power lines. IEEE Trans. Power Electron. 2015, 30, pp. 6191–6202

[14]. Park, B., et al. (2018). "Optimization design of toroidal core for magnetic energy harvesting near power line by considering saturation effect." **8**(5): 056728.

[15]. Y. Zhuang et al., "An improved energy harvesting system on power transmission lines," 2017 IEEE Wireless Power Transfer Conference (WPTC), Taipei, 2017, pp. 1-3.

[16]. P. Maharajan, M. Salauddin, H. Cho, J.Y Park., “An indoor power line based magnetic field energy harvester for self-powered wireless sensors in smart home applications” Applied Energy, vol. 232, December 2018 pp. 398-408,

[17]. Z Wu, D S Nguyen, R M White, P K Wright, G O'Toole and J R Stetter3., “Electromagnetic energy harvester for atmospheric sensors on overhead power distribution lines” IOP Conf. Series 2018

[18]. R. Moghe, Yi Yang, F. Lambert, and D. Divan, “A scoping study of electric and magnetic field energy harvesting for wireless sensor networks in power system applications,” in Proc. 2009 IEEE Energy Convers. Congr. Expo., 2009, pp. 3550–3557.

[19]. K. Tashiro, H. Wakiwaka, S. Inoue, and Y. Uchiyama, “Energy harvesting of magnetic power-line noise,” IEEE Trans. Magn., vol. 47, no. 10, Oct. 2011 pp. 4441–4444.

[20]. C. Jin and H. Chen, “Preliminary electromagnetic analysis of Helium Cooled Solid Blanket for CFETR by MAXWELL," *Fusion Eng. Des.,* Vol. 112, 2016. pp. 468-474,

[21]. D. Giorla, R. Roccella, R. Lo Frano, and G. Sannzzaro, “EM zooming procedure in ANSYS Maxwell 3D,” *Fusion Eng. Des.,* vol. 132, no. April 2018, pp.67-72.

[22]. C. Heneghan, “About the workshop” ANSYS Maxwell 3D 2014 pp. 1-12, 2014.

[23]. ANSYS Maxwell 2013, “Basic Meshing Operations,” pp. 1-19, 2013.

[24]. B. T. Sources, “Basic Transient Sources and Circuit ANSYS Maxwell 3D 2014,” pp.1-23, 2014.

[25]. ANSYS, “Training Manual Lecture 5: Maxwell Transient Solvers,” pp. 1-35, 2013.

[26] I. Said, H. Hussain and V. Dave, "Characterization of magnetic field at distribution substations", 2010 9th International Conference on Environment and Electrical Engineering, 2010.

[27] Jiles, David (1998). Introduction to Magnetism and Magnetic Materials. CRC Press. p. 354. ISBN 978-0-412-79860-3.

[28] Weast, Robert (1983). Handbook of Chemistry and Physics (64th ed.). CRC Press. p. E-108. ISBN 978-0-8493-0464-4.

[29]. Memsic, Wireless Measurement System (MPR2400VB), http://www.memsic.com/userfiles/files/Datasheets/WSN/6020-0060-04- B_MICAz.pdf, 2013

[30]. Invisible-systems, Technical Datasheet: Gateway GPRS, GPS & RF, http://www.invisible-systems.com/solutions/pdf/Gateway%20GPRS%20GPS%20RF.pdf, 2015

APPENDIX A

Investigation on employability of High Magnetic Permeable Materials for energy harvesting application in high voltage power lines magnetic field zone

Hassan Pervaiz[a], Arsalan H. Khawaja[b]1

[a]*USPCASE-NUST, Islamabad, 46000, Pakistan*
[b]*USPCASE-NUST, Islamabad, 46000, Pakistan*

Abstract

Sensing and monitoring is vital for overhead structures such as High Voltage transmission lines (HVTLs) which may be damaged by severe weather conditions and environment, resulting in undesired variation in transmission lines. These sensors need to be continuously powered-up despite hazards. These current carrying conductors generate uncoupled electric and magnetic fields in close vicinity. The aim of this investigation is to analyze various high permeability materials with respect to their efficacy to concentrate the magnetic field when placed near the power lines which will complement the current induction process in the coil of energy harvester. High Magnetic permeable material such as Mu-Metal, silicon Steel and Ferrite were studied in terms of their ability to concentrate the magnetic flux for energy harvesting applications when placed under the region of magnetic field, produced by HVTLs. The modeling and Finite Element Analysis were done using finite Element code program Maxwell 3D from ANSYS which uses Maxwell Equations to solve complex Electromagnetic problems. In this study, different shapes and orientations of these High permeable materials were modeled, simulated and ultimately results were compiled. Mu-Metal showed the most desirable results due to its high ability to concentrate the magnetic flux and hence, induced voltages comparably much more than its other counterparts.

© 2018 Hassan Pervaiz, Arsalan H. Khawaja Selection and/or peer-review under responsibility of Energy and Environmental Engineering Research Group (EEERG), Mehran University of Engineering and Technology, Jamshoro, Pakistan.

Keywords: *Energy Harvesting; Mu-Metal; Magnetic Field; ANSYS Maxwell*

1. Introduction

Energy Harvesting techniques are evolving in recent years, especially with a growing interest in sensor nodes for an Internet of Things (IoT) network. These techniques are

* Dr. Arsalan H. Khawaja. Tel.: +92(0)5190855271.
E-mail address: arsalan@uspcase.nust.edu.pk

being used in wireless sensor networks WSNs, Microelectromechanical systems MEMS and mobile devices. In energy harvesting, ambient energy is scavenged into useful and more compatible energy sources such as Electromagnetic EM Energy is converted into electrical energy. Energy Harvesting is applicable where batteries continuously need to be powered or in areas where human-safety is the main concern. Many harvesting techniques such as Solar, Wind, EM vibration, inductive and capacitive coupling have been researched and applied to relevant and compatible technologies. An EM field is created in the vicinity of AC power lines when a sufficient amount of current is passed through Medium and High Voltage Transmission Lines HVTLs. The magnetic component of EM field is our field of interest which will be used as a source of energy and ultimately will be harvested. Conventionally, energy from Electromagnetic field used to be harvested from current transformers. Inductive coupling is one of the most researched topic to harvest EM field. The authors of paper [1] made one of earliest try to utilize AC power lines current-carrying conductor and inductor combination to induce 412mV. In another research [2], a cylindrical core was made of steel and was placed in the region of 66uT magnetic field of HVTLs and around 300mW of power was harvested. A Mn-Zn ferrite-based bow-tie core was made, having low eddy current losses, high magnetic permeability and low demagnetization factor. Hence it achieved better results than other geometries [3]. A helical core was investigated [4] and determined that it had better performance in terms of power density and efficiency, such that increasing the magnetic flux path and decreasing the demagnetization factor. Rashmi S [5], in his work, modelled different voltage sources and simulated to see the power drawn from them Magnetic flux was also calculated around these sources in MATLAB and Simulink. A Coil-based energy harvester coupled magnetically with alternating current showed the results that AC power of approximately 1.5W can be obtained when the harvester is placed near a power-line conductor carrying a 100 Arms current [6]. In the context of saturating magnetic flux near AC power lines, a toroidal structure was presented that showed effectiveness in inducing voltages [7]. All the literature and research have ultimate motive to concentrate the magnetic flux in the core. Coil purpose is to converge that field into itself and turn into electrical form. The magnetic field may be generated from any source which in our case is 11kV power lines. The theme of research is to investigate the

ferromagnetic materials such as Silicon-Steel, Mu-Metal and Ferrite to show their characteristics of inducing voltages as core and coil when put under the 50/60 Hertz Magnetic field. Voltage induction in coil is the function of Magnetic flux and the materialistic properties of core materials, as suggested by Faraday's Law of induction [8]

$$V_{in} = N\omega B_{ex} A \mu_{eff}$$

Where V_{in} is the AC voltages, N is the number of turns wound on the core, ω is angular frequency, B_{ex} is external magnetic field, A is cross sectional area of the coil and μ_{eff} is the effective permeability of the core material. Effective permeability is the most important part of magnetic flux concentration since it consists of magnetic permeability and the geometry of that material and can ultimately affect the voltage induction.

2. Simulation and Results

ANSYS Maxwell is used as the designing and simulation tool. It performs magnetic modeling using finite element code program called MAXWELL 3D. It is capable to analyze Electromagnetic field problems in Two-Dimension 2D and Three-dimensions 3D where the sources originate from Permanent magnets, external magnetic fields and DC current or voltages. Initially, a 3-phase line of 11kV was designed, having same materialistic properties and parameters such as Voltages and current equations were provided that created the magnetic field in the vicinity of the region.

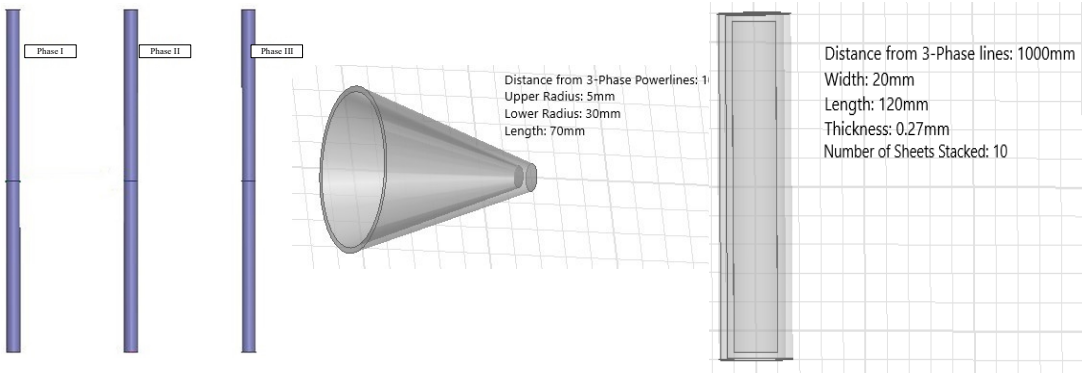

Fig. 1. Designs in Ansys Maxwell (a) 3-Phase 11kV Powerlines in ANSYS Maxwell (b) Cone (c) Stacked Sheets

As can be clearly seen in the figure that, 3-Phase 11kV lines have magnetic field in the region, maximum at the center 10^{-3} Tesla and reduces as the distance increases to

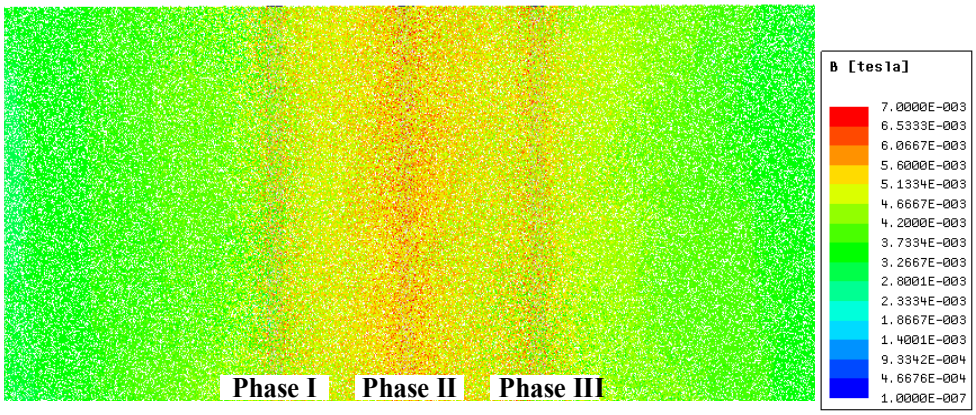

Figure 2: Top view of Magnetic field around 11kV at 0.01s

10^{-6} Tesla. When shapes of different geometries were placed in the region, every material showed different characteristics.

The distance between coil and powerlines was 850mm for every simulation. Distinct geometries, materials and orientation depicted the varying magnetic flux concentrations due to difference in the demagnetizing field in core materials. If the demagnetizing field was reduced, the core's magnetic flux path lengthened, and it induced more voltages than shorter magnetic flux path [9]. Here is the table showing results with varying geometric-shaped ferromagnetic materials and number of turns when placed in the magnetic field region.

2.1. Cone Shaped

Table 1. Comparative Analysis of Cone-shaped Core

Materials	No. of Turns	Magnetic Permeability	Voltages	Branch Current
Mu-Metal	1000	50000	22mV	0.22A
Silicon-Steel	1000	2000-20000	1.66mV	16.5mA
Ferrite	1000	500-2000	36uV	0.35mA

Table 2. Comparative Analysis of Cone-shaped Core

Materials	No. of Turns	Magnetic Permeability	Voltages	Branch Current
Mu-Metal	2000	50000	0.5V	5A
Silicon-Steel	2000	2000-20000	3.32mV	33mA
Ferrite	2000	500-2000	72uV	0.7mA

Cone-shaped coil had upper and lower radius of 5mm and 30mm and length of 70 mm. It was placed from the 3-Phase power lines at the distance of 850mm. Due to

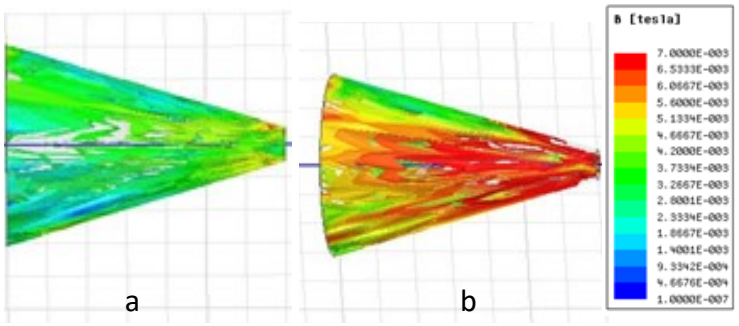

Fig. 3. Magnetic flux in Mu-Metal Cone Geometry (a). 1000Turns (b). 2000Turns

very high magnetic permeability of Mu-Metal, which is specifically designed for the magnetic shielding and flux concentration, results showed much good response than its other counterparts. Conic structure itself increased the path from North to South pole for magnetic field which decreased the demagnetization factors.

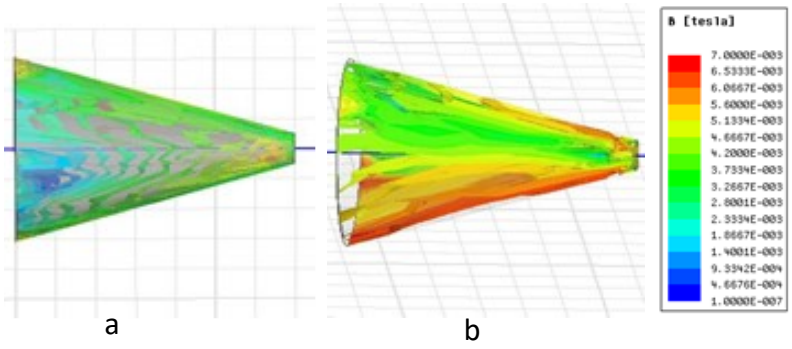

Fig. 4. Magnetic flux in Silicon-Steel Cone Geometry (a). 1000Turns (b). 2000Turns

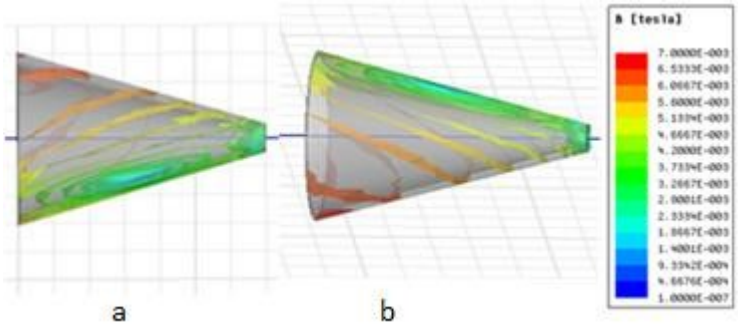

Fig. 5. Magnetic flux in Ferrite Cone Geometry (a). 1000Turns (b). 2000Turns

Every material was in distance of 0.85m from 3-phase lines, had similar inner-outer radius and similar length. Results of table and graphs were in harmony that materials having

good ability to concentrate magnetic flux rendered good results in inducing voltages. And as Magnetic circuit theory suggest, magnetic flux tended to pass through the shortest path where magnetic reluctance was low, which in this case a property largely kept by Mu-Metal, Silicon steel and Ferrite respectively. Mu-Metal, when number of copper turns were increased from 1000 to 2000, showed significant increase in magnetic flux density and hence induced voltages much more than other materials.

2.2. Stacked Sheets

The length, width and thickness of sheets were 100mm, 20mm and 0.27mm respectively. Ten sheets were stacked for simulation purpose because simulation time was increasing on increasing number of sheets.

Table 3. Comparative Analysis of Stacked-Sheets Core

Materials	No. of Turns	Magnetic Permeability	Voltages	Branch Current
Mu-Metal	1000	50000	269mV	2.7mA
Silicon-Steel	1000	2000-20000	0.8mV	0.6mA
Ferrite	1000	500-2000	3.22uV	36uA

Table 4. Comparative Analysis of Stacked-Sheets Core

Materials	No. of Turns	Magnetic Permeability	Voltages	Branch Current
Mu-Metal	2000	50000	128mV	1.3mA
Silicon-Steel	2000	2000-20000	1.66mV	16.5mA
Ferrite	2000	500-2000	1.63uV	15uA

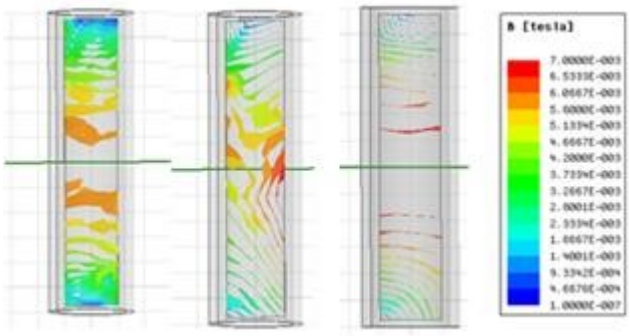

Fig. 6. Magnetic flux in Mu-Metal Stacked-Sheets Core with 1000Turns(a). Mu-Metal (b) Si-Steel (c) Ferrite

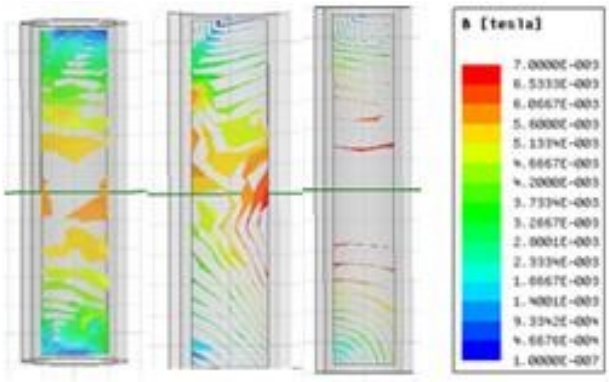

Fig. 7. Magnetic flux in Mu-Metal Stacked-Sheets Core with 1000Turns(a). Mu-Metal (b) Si-Steel (c) Ferrite

With similar parameters set such as conic structure, stacked sheets showed non-linear response. As illustrated in the figures, magnetic flux is not as concentrated as conic because of the reason that linear sheets had higher demagnetizing factor that led to decrease in effective permeability and ultimately lower generation of voltages in the sheets despite using higher permeable materials. Mu-Metal relatively showed better response than others in inducing the voltages. Mu-Metal despite having high magnetic permeability, it saturates at lower magnetic flux of 8000 Gauss, in comparison to Silicon-Steel which saturates at 22000. Since our application is in the region of very low magnetic flux density at 50/60 Hz, Mu-Metal is better candidate to be used as core material.

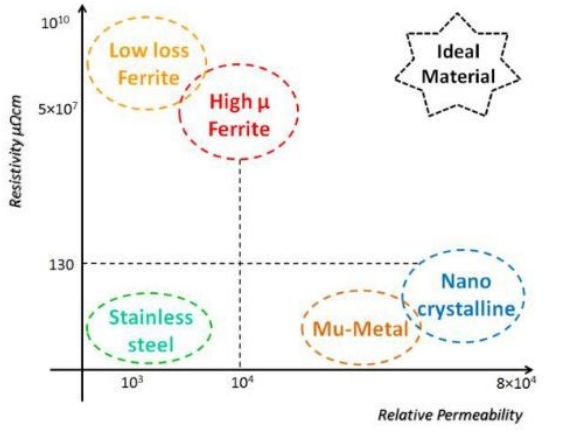

Fig 8. The relative permeability and resistivity of Ferromagnetic materials [10]

3. CONCLUSION

With the above simulation results and calculations, we can conclude that an efficient magnetic material should have good magnetic permeability, lower demagnetization factor, high resistivity and suitable geometry. Mu-metal showed the best response in every geometry under magnetic field region originated by 11kv 3-Phase lines. With advent of inventing and researching a geometry which can more lengthen the path of magnetic field, there will be significant increase in the power density in the energy harvesting. This study can act as promising means for contactless magnetic energy harvesting in overhead medium and high voltage transmission lines. In future, the practical realization of simulation will be carried out.

ACKNOWLEDGMENTS

The authors would like to thank USPCASE-NUST and USAID for supporting this research work.

References

[1]. Gupta V, Kandhalu A and Rajkumar R 2010 Energy harvesting from electromagnetic energy radiating from AC power lines Proc. 6th Workshop on Hot Topics in Embedded Networked Sensors—HotEmNets ’10 pp 1–6

[2]. RM. White, “Atmospheric Sensors and Energy Harvesters on Overhead Power Lines”, Sensors(Basel), 2018

[3]. Yuan, S.; Huang, Y.; Zhou, J.F.; Xu, Q.; Song, C.Y.; Thompson, P. Magnetic field energy harvesting under overhead power lines. IEEE Trans. Power Electron. 2015, 30, 6191–6202

[4] S. Yuan, “A High Efficiency Helical Core for Magnetic Field Energy Harvesting”, IEEE Transactions on Power Electronics, Volume 32, Issue:7,2016 pp. 5365-5376

[5] Rashmi, S, “A Study on Energy Harvesting from Sub-Transmission System to Power Wireless Sensor Nodes”, Grenze, 2017

[6] RM. White, “Atmospheric Sensors and Energy Harvesters on Overhead Power Lines”, Sensors(Basel), 2018

[7] B.Park,D Kim “Optimization design of toroidal core for magnetic energy harvesting near power line by considering saturation effect”, AIP Advances, 2018

[8] S. Yuan, Y. Huang, J. Zhou, Q. Xu and C. Song, “Magnetic Field Energy Harvesting Under Overhead Power Lines”, IEEE Transaction on Power Electronics, Vol. 30, Issue 11, 2015, pp. 6191 – 6202

[9] D. Jiles, “Introduction to Magnetism and Magnetics Materials”, in Magnetism, 2nd ed. Ames, Iowa: Chapman & Hall, 1998, pp. 49-51

[10] S. Yuan, “A High Efficiency Helical Core for Magnetic Field Energy Harvesting”, IEEE Transactions on Power Electronics, Volume 32, Issue:7,2016 pp. 5365-5376

Method for Contactless Energy Harvesting Under Medium and High Voltage Power lines

Hassan Pervaiz[1], Arsalan H. Khawaja[1], and Muhammad Kazim[1]
[1] Center for Advanced Studies in Energy, National University of Science and Technology, Islamabad Pakistan

***Abstract*--The importance of high and medium voltage power lines has drastically increased due to high industrial electricity demand. However, these lines are faced with harsh environments. For this reason, real-time monitoring devices are used to supervise the potential dangers. Real-time data is continuously observed by the monitoring units that are installed in the vicinity of transmission lines. However, these devices are faced with limited battery capacity and the need of convenient and efficient power supply is the need of the time This paper focuses on the optimum energy harvesting method based on magnetic induction phenomena by using the Mu-metal. In this work, magnetic field energy harvester is placed near high voltage (HV) and medium voltage (MV) power lines. It is found that Mu-metal achieves the best magnetic flux concentration and thus is employed in our method. The cone-shaped coil is developed that is used in harvesting of magnetic field energy from HV and MV lines. This new designed coil contributes to the increase in the magnetic flux path that is further used to increase the induced voltages of the coil. By comparing with the recently reported energy harvester designs to be used for power lines, the proposed cone-shaped coil has higher power density of 5.5uW/cm^3.**

***Index Terms*-- Inductive Coil, Magnetic Field, Energy Harvesting, Mu-Metal, Sensors**

I. INTRODUCTION:

With the growing interest in Internet-of-Things (IoT) network, energy harvesting methods have seen exponential growth in this domain. Wireless sensor nodes are used as inexpensive and low-power devices for monitoring and transmission of measured quantities such as temperature, overload, heating, current, and voltage of AC lines in grid and power distribution lines [1]. Power distribution transmission line monitoring is an important issue in power system engineering because 85-87% of power system faults are occurring in transmission lines [2]. For emerging

smart grid application, the high and medium voltage power lines require energy efficient constant monitoring units. These sensors send the real-time data to centralized monitoring units about the condition of AC lines which helps in detecting the potential disasters in early stages.

The conventional sensors are powered by the batteries that have bottlenecks of continuous discharging, regular maintenance and replacement. These constraints urge in finding adequate energy harvesting techniques which can minimize these problems. In order to overcome this existing problem, energy harvesting techniques are combined with existing sensor nodes.

Energy harvesting techniques such as Solar [3], Wind, Piezoelectric [4], inductive [5,6] and electric energy harvesting from power lines [7] have been thoroughly studies and implemented in a number of applications. Although the Solar power technology is very well investigated and many of its product are readily available in the market but the need of adequate weather conditions for extracting power and very low power density of Solar energy has its own conundrums [8]. Likewise, wind energy is the second most widely used renewable energy and have well-established power generation technologies but partial availability of wind source and low power density are major constraints [9].

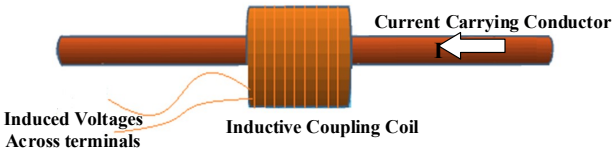

Fig:1 Illustration of CT-Inductive Coupling

The conventional method of energy harvesting from AC power lines utilized the application of current transformer for self-powering of the sensors deployed at the location of transmission lines inductive coil encloses low-diameter power lines as shown in figure 1 [10]. However, CT based inductive coupling requires such devices to be connected to power lines. CT inductive coupling method is not desirable in High voltage power lines because the cross-sectional area of power lines is large as compared to the CT energy harvester core-gap. Another concern with CT-Energy harvester is induction zone of power lines. This method can cause life hazards with high voltage power lines since energy harvester has to be clamped with power lines for inductive coupling. Therefore, it needs to take safety concerns into consideration. To overcome the issue, the concept of contactless energy was introduced where energy harvester is placed at the distance from HV lines. Contactless energy harvesting solutions are preferred over conventional methods. Such methods are not only helpful in providing safe distance to the line personnel that allows him to work outside induction zone of energized HV power lines but also ensures the protection of the device itself. Several studies have been done on contactless inductive coupling and these studies have been used in powering the wireless sensor nodes and batteries at the power lines and the smart grid.

In paper [11], researchers designed coil of cylindrical shape with a steel core and harvested 300mW when placed in magnetic field of 66uT. Similarly, Yuan et al [12] proposed Mn-Zn Ferrite based Bow-Tie coil, with 40000 turns and placed it under 7uT, achieving power of 146.7mW and power density of 1.86uW/cm^3. Roscoe et al made a 50cm long solenoid and achieved 0.845uW/cm^3 under substation magnetic field of 18.5uT [13]. In another work, Researchers modelled a helical coil of 15cm with core having magnetic permeability of 100,000 under 7uT to achieve power of 2.86mW and induced voltages of 910mV [14]. All this work is distinguished by using ferromagnetic materials with varying magnetic permeability, geometries, number of turns and orientations. These designs are

This paper presents the novel mu-metal contactless magnetic field energy harvester, using Mu-Metal as a core material with high magnetic permeability. Cone-shaped design overcomes the constraint of complexity of coil design and ensures maximum magnetic flux concentration in coil. This combination increased the magnetic flux density as well as enhanced power density in small volume.

The section II consists of The Energy Harvester design which give details about Theory, Finite Element Analysis and Physical Design. Section III comprises of proposed coil experimentation. Section IV and V includes energy harvesting circuit and coil comparative analysis with other designs. Paper. The conclusion is given in section VI.

II. The Energy Harvester Design

A. Theory

In a contactless energy harvesting technique, a coil is made up of ferromagnetic materials that has capability to convert the magnetic field energy that lies around HV lines into electrical energy. Previous designs used the ability of ferromagnetic core materials to concentrate the magnetic field so that its magnetic flux path is increased, which ultimately causes the coil to induce voltages. Our study focusses to the part on optimizing the suitable core material and design that increase the magnetic flux path and inducing voltages according to the Faraday's law of induction [12].

$$V_{in} = N\omega B_{ex} A u_{eff} \qquad (1)$$

Where V_{in} is the voltages induced by the coil, N is the number of copper winding turns around the core, B_{ex} is the external magnetic field around the transmission lines, ω is the angular frequency of B in terms of

radian/sec, A is the effective area of the coil and u_{eff} is effective permeability of coil which is normally related to the magnetic permeability of core material and geometric shape.

The core design mainly depends upon the effective permeability u_{eff}, that is further sub-divided into materialistic property and the geometry. High effective permeability leads to high voltage induction and ultimately to higher power density of a coil. A coil achieves higher effective permeability when the core allows a lengthy magnetic flux path from the north pole to the south pole. A demagnetizing factor D_M is geometry-dependent parameter which increases with the increase in the demagnetizing field H_D and decreases with increase in the magnetization *M* of the core where demagnetization field is the resistive tendency to magnetization of a geometry and affect the total magnetic field concentration in the core [15]. The demagnetization field H_D mainly depends upon the type of ferromagnetic material and the geometry of core and can be calculated by equation 2:

$$D = H_D / M \qquad (2)$$

To have maximum flux concentration in a design, magnetization field should be higher than the demagnetization field.

Inductive coils show similar characteristics when they are placed under magnetic field of certain frequency. Figure 2 shows the equivalent diagram of inductive energy harvester operating at 50Hz. Induced voltages of coil are function of its properties and the external magnetic field. The total coil resistance is equivalent to core resistance and the copper winding resistance. According to the maximum power transfer theory, a coil inductance which is a factor that resist the flow of current through coil, is minimized by placing a compensating capacitor and the matched load RL which should have value of total coil resistance to ensure that maximum power is transferred.

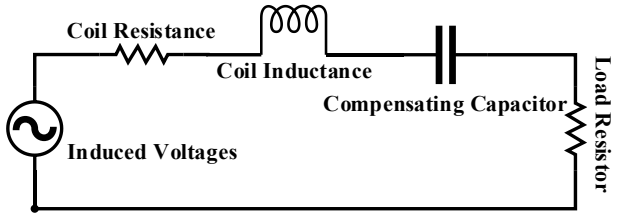

Fig 2: Equivalent Energy Harvesting Coil at 50 Hz frequency

The power at the load resistor is dependent on induced voltages and the total coil resistance under magnetic field region and it is calculated by using equation 3 [12]:

$$P = \left(V_{coil} / 2\right)^2 / R_{coil} \qquad (3)$$

The power density of inductive coil (power output per unit volume), under these attributes, can be calculated from the equation 4 [12]:

$$S_{power} = 0.25 \left(V_{coil}{}^2 / R_{coil}\right) / Vol_{coil} \qquad (4)$$

The equation suggests that power density is not solely dependent upon induced voltages but also on Coil resistance under magnetic field and the volume of the coil. Vcoil is coil's open circuit voltage, Rcoil is the total effective coil resistance and is combination of total wire and core resistance in ohms and Volcoil is total volume occupied by the coil in m^3.

Since the coil will be placed under the power lines for inductive coupling, it is important to understand the flow of electric current in power lines that creates magnetic field in its close vicinity. The frequency of magnetic field in the region of power lines is 50/60Hz depending upon the power system used. The strength of magnetic field is in order of uT (10^{-6} Tesla), highest at the center and decays as distance from the center increases. Proportional to intensity of magnetic field, an inductive coil, made up of ferromagnetic material that have a certain magnetic permeability, is wound by copper wire and is placed under magnetic field. Intensity of induced voltages is directly proportional to the magnitude of magnetic field. It can be inferred

that induced voltages are the function of coil properties and external magnetic field surrounding the coil [12].

Using the parameters stated in Faraday's law and demagnetization factor, a coil was initially simulated and designed in the environment of MV power lines (11kV) by Finite Element Analysis Method.

B. Finite Element Analysis

FEA is used to optimize power delivery by voltage induction in a coil. This requires optimizing material properties, its orientation and geometric shape with respect to power lines configuration. ANSYS Maxwell Electromagnetism was used which is the designing and simulation tool and perform magnetic modeling using finite element code program called MAXWELL 3D. The FEA was conducted using open-circuit configuration under air region. For investigation on placement of energy harvesting in power distribution, one-circuit three phase power distribution was selected. As shown in figure 3(a), 11kV power system was designed and three conductors were given current values of 3-phase 11kV as described in the equation 2. At origin, 3-phase lines produced magnetic field of 7mT and as the distance increased from the power lines, the magnetic flux density decreased. An 11kV power lines produced 10-12uT, figure 3b, at the distance of 1 meter that has verified the study [16]. Moreover, simulations were done in the magnetic transient solvers that compute magnetic field with time varying mode. Three phase current is represented by the following equation 5:

$$I = \sqrt{2} I_{rms} Sin(\omega t \alpha) \qquad (5)$$

where I_{rms} is the current variable passing through conductors of 11kV lines, ω is angular velocity which is equal to 2πf and α is defined in degrees ±120. The Phase1, Phase2 and Phase 3 would be put in equations as +120, -120 and 0 degrees, respectively.

A coil was made with geometries like rectangular sheets, cylindrical and Cone by using different ferromagnetic materials such as Ferrite, Silicon-Steel and Mu-Metal as shown in figure 4. Mu-Metal has the highest magnetic permeability (ur~60000-100000) among Ferrite (2000-10000) and Si-Steel (2000-20000) and simulation results verified that magnetic flux concentration is better for materials that has higher magnetic permeability.

Rectangular sheets core, with thickness of 0.25mm, length of 80mm and width of 2 cm, were stacked upon each other and were simulated. Figure 4 shows that rectangular stacked sheet's ability to extend the magnetic flux is the best in Mu-Metal, followed by Silicon steel sheet and Ferrite Sheet. The magnetic flux line passing through rectangular sheets in all three sheets is low, that shows in visualization the demagnetizing factor of the core design which ultimately results in low voltage induction.

A cylindrical shaped coil was also simulated and investigated under same circumstances as Rectangular sheets. The length of coil was kept 15cm with 5cm of radius and was placed at the distance of 1000mm. Figure 4 also illustrates the response of cylindrical cone under magnetic field. The effective area of coil with magnetic flux is better than rectangular sheets. However, the number of magnetic flux lines are higher than rectangular sheets which indicates that there is lower demagnetization factor in the geometry than rectangular sheets. But among Mu-Metal, Silicon-Steel and Ferrite, as in rectangular sheets, Mu-metal is the most suitable material for magnetic flux concentration.

For further analysis, to investigate ferromagnetic materials and design, a truncated cone-shape coil was simulated. Simulation of cone-shaped design showed better results of magnetic flux concentration as compared to rectangular sheets and cylindrical core design. Effective area of cone-coil under magnetic field is larger than previous designs. Among three materials, Mu-Metal cone coil had the lowest demagnetization factor which allowed larger magnetic field to pass through the design. The magnetic flux inside the cone-coil was visualized in order of 3-7mT. It was visually realized that magnetic flux concentration was maximum at the center and lower at the both ends. Table 1 depicts the number of magnetic flux lines passing through different core designs of ferromagnetic materials. The results verify that Mu-Metal cone-core concentrated the most magnetic field line, followed by silicon steel cone-core. On comparison of all three designs and materials, it can be stated that Mu-Metal cone should be used for making inductive coil.

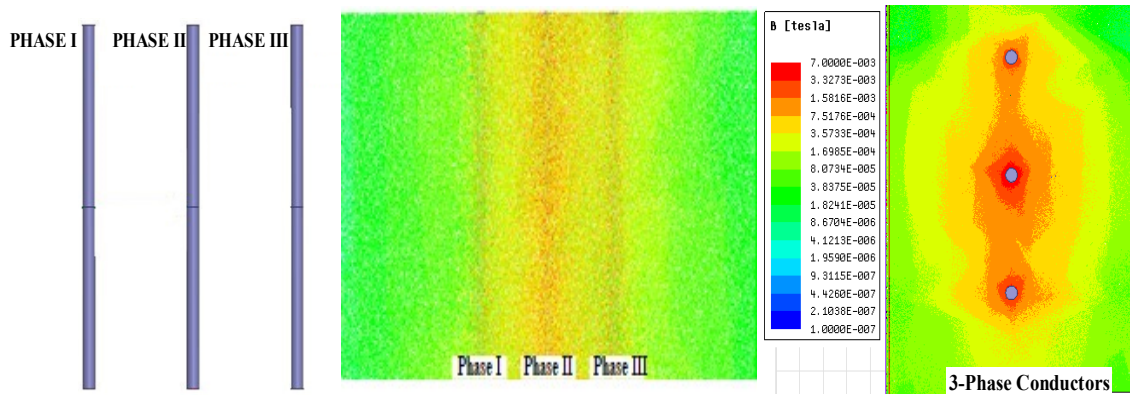

(a) (b) (c)

Fig 3: 11kV power system a) Top View of 3-Phase 11kV conductors in ANSYS Maxwell b) Top view of Magnetic field around 11kV at 0.01s c) Side view of MF around 11kV at 0.01s

TABLE I
MAGNETIC FLUX LINES IN SIMULATED CORES IN TESLA

Ferromagnetic Materials	Cone-Core	Cylindrical Core	Rectangular Core
Mu-Metal	0.0032	0.0027	0.0021
Silicon Steel	0.0028	0.002	0.0019
Ferrite	0.0021	0.0015	0.0015

Induced voltages have direct relationship with core air-gaps because air gaps allow the demagnetization factor to reside in the coil design which ultimately cause reduced flux-linkage with the coil. This reduced flux-linkage further cause reduction in voltages induction. In simulation, a perfect cylindrical and truncated-cone were simulated which were free of any air gaps but in practical, it is difficult to make cone shape cores from metal sheets without air gaps.

C. Physical Design

After optimization of the coil design and material in ANSYS Maxwell, a physical coil was designed. Cone-Coil tends to have many layers of cone-shaped Mu-Metal, stacked to increase the width and the magnetic permeability of core. The core air-gap needs to be low to achieve better number of induced voltages. Despite having high magnetic permeability, Mu-Metal has drawback of having low magnetic saturation and low resistivity in the order of 10Ω which in comparison to ideal material should be very high of order 10^{10}Ω. Another reason to choose Mu-Metal despite having low resistivity of 60μΩcm and low saturation of 8000Gauss, as compared to Silicon steel which has high saturation level of 22000 Gauss, is availability of very low magnetic field density under MVTLs and HVTLs, in uT with 50/60Hz frequency. This low intensity of magnetic field is insufficient to saturate the core that makes it desirable for applications under medium and high voltage power lines.

A Mu-Metal sheet of 0.24mm thickness and magnetic permeability of approximately 60000, was molded into the cone shape. The height, lower radius and upper radius of cone-core was 8cm, 2cm and 3cm respectively. A cone was also designed in Ultimaker software and printed from 3D printer to give stability while winding of copper wire on cone-shaped Mu-Metal layers as shown in Figure 5.

SWG-32 enameled copper wire was chosen for winding around the core which had diameter of 0.274mm and resistivity of 0.292 Ω/m. The chosen enameled wire was smaller in diameter as it gives more turns on fixed core volume which ultimately causes more induced voltages. Coil has its own internal core and wire resistance. Core resistance does not account until it is placed under the magnetic field region. It is also desirable that coil resistance should be equal to wire resistance. This makes core resistance to be negligible which is made sure during designing the cone-coil. The wire resistance was 225Ω at 4000 copper turns. Wire resistance are calculated by Multi-Meter It is important to choose a wire that can deliver the maximum

power whereas also keeping the resistance of coil as minimum as possible because enameled wire directly affects the coil resistance, power and power density. Figure 6 illustrates the cone coil resistance upon increasing the number of turns.

III. Coil Experimentation

Coil was tested in lab by Helmholtz coil which was externally powered up by waveform generator at the 50Hz frequency. The magnetic flux density of Helmholtz coil can be calculated by the [17]:

$$B_{Helmholtz} = (0.8)^{3/2} \mu_o NI / R_H \qquad (5)$$

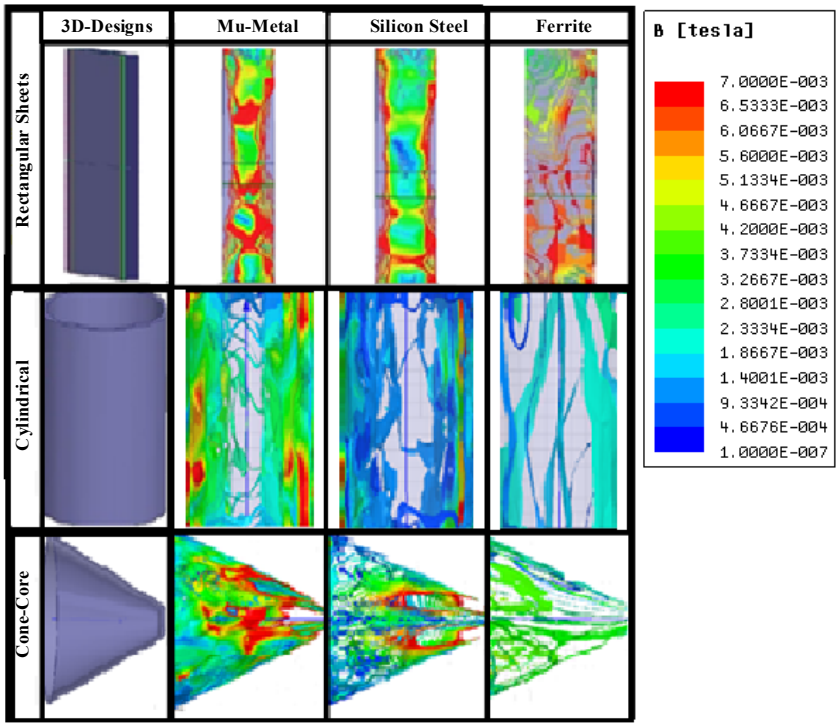

Fig 4: Graphic illustration of magnetic flux concentration in core shaped materials

(a) (b) (c)

Fig 5: Design of cone-coil for experimental setup (a) 3D-Cone Design in Multimaker for printing (b) Printed 3D-cone and one-layer of mu-metal core (c) Final cone-shaped core with coil

where μ0 is the vacuum permeability, N is the number of turns, I is the current passing through the coil and RH is the radius of the Helmholtz coil. Helmholtz coil, in this experiment, is given 300 copper turns and with radius of 0.1m. The pairs of coil are separated by the distance of their radius. A current of 5.5mA is passed through the coils. Magnetic field density of 15uT was generated by Helmholtz at the center.

Figure 6(a) shows open-circuit configuration of cone-coil. Coil is placed between the Helmholtz coil in magnetic field density of 15uT. Oscilloscope shows the open-circuit induced voltages in the form of sinusoidal form. In figure 6(b), the experimental setup is shown where coil is placed between the Helmholtz coil and Cone-coil is further connected to Energy Harvesting circuit. Digital Multimeter measured the DC voltages at the end of circuit.

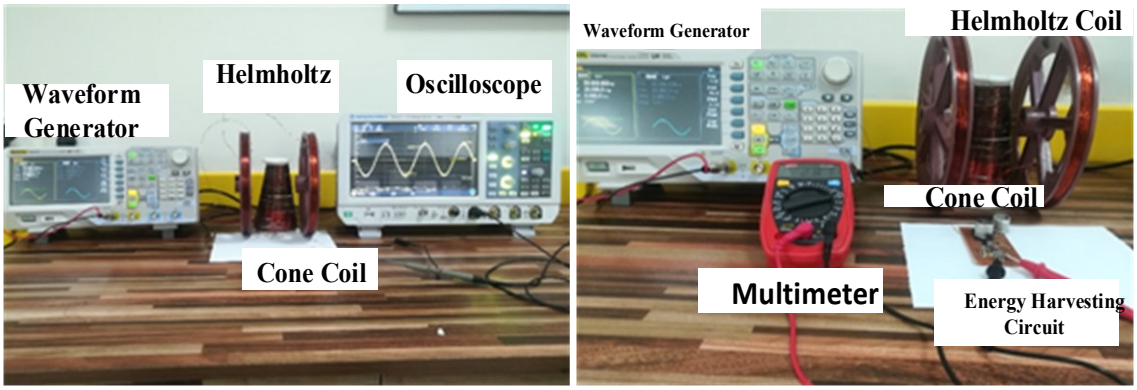

(a) (b)

Fig 6: Energy Harvesting system testing a) No-load voltage visualization b) Short-circuit current measurement

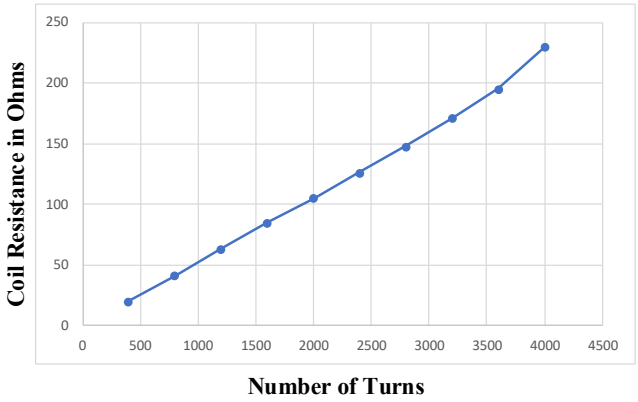

Fig 7: The effective coil resistance without placing under magnetic field as function of winding numbers

Table II summarizes the response of a single Mu-metal layer of cone-shape coil when layers of copper winding are gradually increased. The induced voltages gradually increase to 300mV at 3000 turns. Since thick core tends to have higher induced voltages, number of layers are increased to 2,3,4 and 5 which in response induced 420mV, 590mV, 770mV, and 1V respectively at 3000 turns under 15uT magnetic field as shown in table 3. This proves the concept that on increasing the core width, there is more concentration of magnetic flux, lesser demagnetization factor and more flux linkage which ultimately gives the results in better voltage induction. For experiments, the 5-layers of Mu-Metal, to increase the thickness, is used to prove the concept as further increasing the core layers would make coil heavy and expensive which is undesirable. When copper turns were increased from 3000 to 3950. The coil induced 1.25V on placing at the magnetic field strength of 15uT.

TABLE II: INDUCED VOLTAGES WHEN SINGLE-LAYERED MU-META LCOIL WAS PLACED UNDER 15UT MAGNETIC FIELD

N (Number of turns)	Vin (Voltages Induced)
240	35mV
480	65mV
1200	130mV
2400	250mV
3000	300mV

TABLE III: INDUCED VOLTAGES WHEN COIL AT 3000 COPPER TURNS WAS PLACED UNDER 15UT MAGNETIC FIELD AT DIFFERENT LAYERS

Mu-Metal Layers n	Induced Voltages
2	420mV
3	590mV
4	770mV
5	1000mV

Figure 8 shows the relation between number of turns and the induced voltages of a larger cone-coil. A linear trend can be seen that with every 400 turns, an approximately 0.1V were increased.

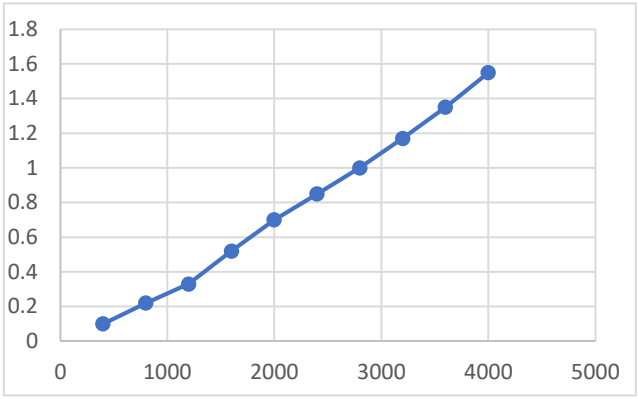

Fig 8: The 5-layered Cone-coil induced voltages as function of winding numbers

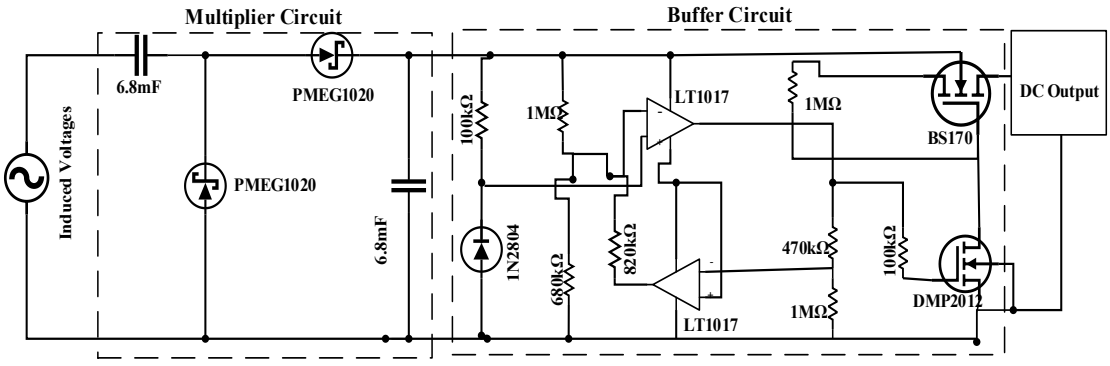

Fig 9: Energy Harvesting Circuit

A regular sinusoidal sine wave is generated to show that induced voltages are in AC waveform with a little distortion. Voltage induction increased when coil is placed to a stronger magnetic field region.

IV. Energy Harvesting Circuit

Since the output voltages need to be in pure DC form to function the end device i.e. sensor nodes, induced voltages which are in AC form, were to be rectified in DC voltages. For this purpose, coil was connected with a Cockroft-Walton multiplier circuit that functions like a rectifier circuit, converting AC voltages to DC, which also boost up the rectified voltages according to the number of stages of multiplier circuit. Here a double-stage multiplier circuit was used that adds the peak-to-peak voltages. Since normal Germanium and Silicon diodes drop the voltages from 0.3V to 0.7V respectively, it is undesirable to use these diodes in multiplier circuit. Instead, Schottky diodes PMEG1020EA with voltage drop of 0.1V and capacitors of 6.8mF were chosen for the construction of Multiplier circuit [18]. The multiplied DC output voltages were actually input peak voltages minus the voltage drop across diodes, which in the case of this circuit was of 1V DC. Multiplier circuit was further connected with the buffer circuit. Buffer circuit cut off the supply from coil to DC-DC converter, once the sufficient voltages were not supplied by coil or specifically when there was insignificant magnetic flux linkage to the coil. The buffer circuit was formed by LT1034, current comparator LT1017 and MOSFET switches as proposed in the research [7]. Some voltages were consumed in powering up the buffer circuit which ultimately gave output of 650mV of DC voltages when capacitors were fully charged. Figure 9 shows the circuit diagram of Energy harvesting circuit.

V. Results and Comparative Analysis:

The Mu-metal cone coil has able to harvest energy from magnetic field. It proved the concept of Faraday's law of induction and induced voltages accordingly. The main consideration of investigation was to improve the effective permeability part of Faraday's law and that was achieved by designing the cone-coil. Volume of coil was kept comparative to the previous designs. By using the equation 2 and equation 3, power and power density of coil was calculated. Cone-Coil shaped achieved total power density of 5.5uW/cm^3 at the magnetic field region of 15uT and with matched-load, coil transmitted the power of 4.34mW.

Table 4 gives a detailed comparison of coil parameters of Cone-Coil with other studies and designs. The cone-coil occupies less space than Solenoid Coil and Bow-Tie Coil. Cone-coil is also simpler in design, easy-to-make and efficient than previous designs. The total wire resistance was 215Ω but when placed under magnetic field region, the total measured coil resistance decreased to 90ohms which on comparison with Solenoid coil is very less. Total helical coil resistance would have been higher than Cone-shaped if copper turns of helical coil would be increased.

TABLE: IV Comparative analysis of coil parameters of different design methods

Coil Parameters	Helical Coil [14]	Solenoid Coil [7]	Proposed Cone-Coil	Bow-Tie Coil [12]
Length	15cm	50cm	13cm	15cm
Magnetic Flux	7uT	18.5uT	15uT	7uT
No. of Turns	400	40000	3950	9500
Wire Diameter	0.4mm	N/A	0.274mm	0.14mm
Voltages Induced	185mV	10.5V	1.25V	0.73
Coil Resistance	13.96Ω	33kΩ	90Ω	160.2Ω
Coil Volume	292cm^3	981cm^3	450cm^3	800cm^3
Coil Power	612uW	833uW	4.34mW	0.831mW
Power Density	2.1uW/cm^3	0.85uW/cm^3	5.5uW/cm^3	1.86uW/cm^3

Voltage induction would have been much better if core layers were without air-gaps. The air-gaps led towards less magnetic flux linkage. Proper machine winding of copper wire on core would have made positive impact on induced voltages since manual winding caused improper and misaligned coverage on core. Results can be improved if these parameters are accounted properly while designing the coil. However, the coil manages to have the better power and power density than previous designs and almost two times better than the Helical coil. If the number of Mu-Metal layers and length of coil are increased, there will be more path for magnetic flux and coverage for copper wire. At the length of 20cm, 7 Mu-metal layers and 10000 turns, it is predicted that induced voltages will be increased to 5V and power density to 20uW/cm^3.

VI. Conclusion:

An innovative, simple and novel coil design of cone shape is discussed in this paper that can harvest energy when placed in the region of magnetic field, generated by high voltage transmission lines. By the method of inductive coupling, the coil is able to induce voltages without being connected to the. Finite Element Analysis showed that Mu-Metal is the best choice for ferromagnetic core material among Ferrite and Silicon Steel. Cone design was proclaimed as the geometry of the coil. A Cone shaped coil was physically designed and experimented. The coil was 13cm in length and was given 3950 turns of copper enameled wire. Coil was able to induced 1.25V under the magnetic field density of 15uT. Uniform magnetic field region was generated by the Helmholtz coil. Coil was further connected with the energy harvesting circuit that rectified the induced voltages for the compatibility of end devices. With matched-load, coil could harvest 4.5mW and the power density of 5.5uW/cm^3. The results proved that cone coil had better power density than Helical, Bow-tie and Solenoid designs. Power density can be estimated to go as high as 20uW/cm^3 if length of coil is increased to 20cm, number of Mu-Metal layers to 7 and turns are increased to 10000. The total power output also can be increased to 100mW when cone-coil is placed to higher magnetic field region of 25uT that is enough to power the low-power sensor nodes efficiently.

Acknowledgments:

The authors are thankful to USAID and USPCASE for funding the research.

References:

[1]. M. Erol-Kantarci and H. Mouftah, “Suresense: sustainable wireless rechargeable sensor networks for the smart grid,” IEEE Wireless Commu., vol. 19, no. 3, pp. 30–36, June 2012.

[2]. Manohar singh, Dr. B.K Panigrahi, Dr. R. P. Maheshwari, “Transmission Line Fault Detection and Classification”, PROCEEDINGS OF ICETECT 2011.

[3]. Vijay Raghunathan; A. Kansal, J. Hsu, J. Friedman, Mani Srivastava, “Design considerations for solar energy harvesting wireless embedded systems,” Information Processing in Sensor Networks, 2005, pp. 457-462

[4]. G.K Ottman, H.F Hofmann, A.C. Bhatt, G.A. Lesieutre, “Adaptive piezoelectric energy harvesting circuit for wireless remote power supply,” IEEE Trans. Power Electronics, Vol. 17, Issue: 5 2002, pp. 669-676

[5]. R.H. Bhuiyan, R.A. Dougal, M. Ali, “A Miniature Energy Harvesting Device for Wireless Sensors in Electric Power System,” IEEE Sensors Journal, Vol. 10, Issue: 7, 2010, pp. 1249-1258

[6]. N. M. Roscoe, M. D. Judd, "Harvesting energy from magnetic fields to power condition monitoring sensors", *IEEE Sens. J.*, vol. 13, no. 6, pp. 2263-2270, 2013

[7]. J. C. Rodriguez, G. Holmes and B. McGrath, “Maximum energy harvesting from medium voltage electric-field energy using power line insulators” Australasian Universities Power Engineering Conference, AUPEC 2014 - Proceedings. 10.1109/AUPEC.2014.6966633.

[8]. J. A. Paradiso and T. Starner, “Energy Scavenging for Mobile and Wireless Electronics”, IEEE Pervasive Computing, Vol. 4, 2005, pp.18-27

[9]. S. Cao and J. Li, “A survey on ambient energy sources and harvesting methods for structural health monitoring applications” Advances in Mechanical Engineering2017, Vol. 9(4) 1–14 2017

[10]. OTLM Overhead Transmission Line Monitoring system, OTLM 7100, http://www.otlm.eu/en/otlm_device, Accessed Jan 2013

[11]. Gupta V, Kandhalu A and Rajkumar R 2010 Energy harvesting from electromagnetic energy radiating from AC power lines Proc. 6th Workshop on Hot Topics in Embedded Networked Sensors—HotEmNets ’10 pp 1–6

[12]. Yuan, S.; Huang, Y.; Zhou, J.F.; Xu, Q.; Song, C.Y.; Thompson, P. Magnetic field energy harvesting under overhead power lines. IEEE Trans. Power Electron. 2015, 30, 6191–6202

[13]. N. M. Roscoe and M. D. Judd, “Harvesting Energy from Magnetic Fields to Power Condition Monitoring Sensors”, IEEE Sensors Journal, Vol. 13, Issue: 6, 2013, pp. 2263-2270

[14]. S. Yuan, “A High Efficiency Helical Core for Magnetic Field Energy Harvesting”, IEEE Transactions on Power Electronics, Volume 32, Issue:7,2016 pp. 5365-5376

[15] D. Jiles, “Introduction to Magnetism and Magnetics Materials”, in Magnetism, 2nd ed. Ames, Iowa: Chapman & Hall, 1998

[16]. I. Said, H. Hussain and V. Dave, "Characterization of magnetic field at distribution substations", 2010 9th International Conference on Environment and Electrical Engineering, 2010.

[17]. E. Javor and T. Anderson, "Design of a Helmholtz coil for low frequency magnetic field susceptibility testing", 1998 IEEE EMC Symposium. International Symposium on Electromagnetic Compatibility. Symposium Record (Cat. No.98CH36253).

[18]. H. Bhuiyan, R. A. Dougal and M. Ali, "A Miniature Energy Harvesting Device for Wireless Sensors in Electric Power System," in IEEE Sensors Journal, vol. 10, no. 7, pp. 1249-1258, July 2010. doi: 10.1109/JSEN.2010.2040173